

# Network reconstruction for trans acting genetic loci using multi-omics data and prior information

Johann S. Hawe<sup>1,2</sup>, Ashis Saha<sup>3</sup>, Melanie Waldenberger<sup>4</sup>, Sonja Kunze<sup>4</sup>,  
Simone Wahl<sup>4</sup>, Martina Müller-Nurasyid<sup>5,6,7,8</sup>, Holger Prokisch<sup>9</sup>, Harald  
Grallert<sup>4,10,11</sup>, Christian Herder<sup>12,11,13</sup>, Annette Peters<sup>10</sup>, Konstantin  
Strauch<sup>5,7,14</sup>, Fabian J. Theis<sup>1,15</sup>, Christian Gieger<sup>4,10,11</sup>, John Chambers<sup>16,17</sup>,  
Alexis Battle<sup>3,18</sup>, and Matthias Heinig<sup>1,2,\*</sup>

<sup>1</sup>*Institute of Computational Biology, German Research Center for Environmental Health, HelmholtzZentrum  
München, Neuherberg, Germany*

<sup>2</sup>*Department of Informatics, Technical University of Munich, Garching, Germany*

<sup>3</sup>*Department of Computer Science, Johns Hopkins University, Baltimore, Maryland, USA*

<sup>4</sup>*Research Unit of Molecular Epidemiology, German Research Center for Environmental Health, HelmholtzZentrum  
München, Neuherberg, Germany*

<sup>5</sup>*Institute of Genetic Epidemiology, German Research Center for Environmental Health, HelmholtzZentrum  
München, Neuherberg, Germany*

<sup>6</sup>*IBE, Faculty of Medicine, LMU Munich, 81377 Munich, Germany*

<sup>7</sup>*Institute of Medical Biostatistics, Epidemiology and Informatics (IMBEI), University Medical Center, Johannes  
Gutenberg University, Germany*

<sup>8</sup>*Department of Internal Medicine I (Cardiology), Hospital of the Ludwig-Maximilians-University (LMU) Munich,  
Munich, Germany*

<sup>9</sup>*Institute of Human Genetics, School of Medicine, Technische Universität München, Munich, Germany*

<sup>10</sup>*Institute of Epidemiology, German Research Center for Environmental Health, HelmholtzZentrum München,  
Neuherberg, Germany*

<sup>11</sup>*German Center for Diabetes Research (DZD), Neuherberg, Germany*

<sup>12</sup>*Institute for Clinical Diabetology, German Diabetes Center, Leibniz Center for Diabetes Research at Heinrich  
Heine University, Düsseldorf, Germany*

<sup>13</sup>*Division of Endocrinology and Diabetology, Medical Faculty, Heinrich Heine University, Düsseldorf, Germany*

<sup>14</sup>*Chair of Genetic Epidemiology, IBE, Faculty of Medicine, LMU Munich, Munich, Germany*

<sup>15</sup>*Department of Mathematics, Technical University of Munich, Garching, Germany*

<sup>16</sup>*Department of Epidemiology and Biostatistics, MRC-PHE Centre for Environment and Health, School of Public  
Health, Imperial College London, London, UK*

<sup>17</sup>*Lee Kong Chian School of Medicine, Nanyang Technological University, Singapore 308232, Singapore*

<sup>18</sup>*Department of Biomedical Engineering, Johns Hopkins University, Baltimore, Maryland, USA*

\* *To whom correspondence should be addressed*

35 May 19, 2020

36 **Abstract**

37 **Background:** Molecular multi-omics data provide an in-depth view on biological  
38 systems, and their integration is crucial to gain insights in complex regulatory processes.  
39 These data can be used to explain disease related genetic variants by linking them  
40 to intermediate molecular traits (quantitative trait loci, QTL). Molecular networks  
41 regulating cellular processes leave footprints in QTL results as so-called *trans*-QTL  
42 hotspots. Reconstructing these networks is a complex endeavor and use of biological  
43 prior information has been proposed to alleviate network inference. However, previous  
44 efforts were limited in the types of priors used or have only been applied to model  
45 systems. In this study, we reconstruct the regulatory networks underlying *trans*-QTL  
46 hotspots using human cohort data and data-driven prior information.

47 **Results:** We devised a strategy to integrate QTL with human population scale  
48 multi-omics data and comprehensively curated prior information from large-scale bio-  
49 logical databases. State-of-the art network inference methods applied to these data and  
50 priors were used to recover the regulatory networks underlying *trans*-QTL hotspots. We  
51 benchmarked inference methods and showed, that Bayesian strategies using biologically-  
52 informed priors outperform methods without prior data in simulated data and show  
53 better replication across datasets. Application of our approach to human cohort data  
54 highlighted two novel regulatory networks related to schizophrenia and lean body mass  
55 for which we generated novel functional hypotheses.

56 **Conclusion:** We demonstrate, that existing biological knowledge can be leveraged  
57 for the integrative analysis of networks underlying *trans* associations to deduce novel  
58 hypotheses on cell regulatory mechanisms.

59 **Keywords:** systems biology, omics, data integration, network inference, prior information, simulation,  
60 machine learning, personalized medicine

## 61 Background

62 Genome-wide associations studies (GWAS) have been tremendously successful in discover-  
63 ing disease associated genetic loci. However, establishing causality or obtaining functional  
64 explanations for GWAS SNPs is still challenging. In recent years, the focus has shifted from  
65 discovery of disease loci to mechanism and explanation, and large efforts have been put  
66 into unravelling the functional consequences of GWAS SNPs [1, 2]. These have been made  
67 possible through technological advances in measuring genome-wide molecular data in large  
68 population cohorts, which further led to a steady increase in biological resources providing  
69 simultaneous measurements of different molecular layers (often termed *multi-omics* data).  
70 To elucidate disease mechanisms, systems genetics approaches seek to link GWAS SNPs to  
71 intermediate molecular traits by identifying quantitative trait loci (QTL) [3, 4], for example  
72 for gene expression levels (eQTL) [5–7] or DNA methylation at CpG dinucleotides (meQTL)  
73 [8–10].

74 Genetic variants that are QTL for quantitative molecular phenotypes that reside on a  
75 different chromosome are called *trans*-QTL. Previously, *trans*-QTL studies were successful  
76 in model systems [11, 12]. Recently, large-scale meta analyses of molecular QTL in very  
77 large sample sizes have now been applied to successfully map large numbers of *trans*-QTL  
78 in humans [7]. These are particularly interesting, as they have been found to be enriched for  
79 disease associations [7, 8, 13]. Yet, the underlying mechanisms leading to such associations  
80 can usually not be explained in a straightforward way [6], and in fact, 83% of discovered  
81 *trans*-eQTL in human are estimated to still be unexplained [7].

82 *Trans*-QTL hotspots [14], where a single genetic locus influences numerous quantitative  
83 traits on different chromosomes, can be seen as footprints of regulatory molecular networks  
84 and likely encode master regulators. One way of mechanistically explaining the effects of  
85 these master regulators is by reverse engineering the regulatory networks, and hence de-

86 terminating the intermediate molecular processes giving rise to the observed *trans* effects,  
87 ultimately yielding novel insights into disease pathophysiology [1, 14–16].

88 A large body of work has focused on inferring regulatory interactions from high-throughput  
89 data by individually combining distinct genomic layers like gene expression levels and geno-  
90 type [6, 17–19] or chromosomal aberration [20] information. Generally, network inference to  
91 uncover regulatory mechanisms in biological systems has gotten much interest [15, 21–24].  
92 The emergence of multi-omics data now also allows for establishing networks across more  
93 than two omics layers in a holistic approach to obtain more insight into the function of reg-  
94 ulatory elements [16]. Major efforts have been made to recover functional interactions from  
95 such data, but methods to successfully reverse engineer regulatory networks across multiple  
96 omics layers are still lacking [1, 4, 25, 26].

97 Furthermore, utilizing the wealth of data available from genomic databases as biological  
98 prior information can guide the inference of complex multi-omics networks [26–28]. For  
99 instance, using known relationships discovered in previous studies as prior knowledge, such  
100 as protein-protein interactions (PPIs) or eQTL, can facilitate network reconstruction on  
101 novel datasets. Application of priors has been investigated in numerous works [e.g. 15, 27,  
102 29–34], and while several studies show the advantage of using priors in synthetic datasets  
103 [22, 31, 33, 34] or model systems [15, 32, 34, 35], relatively few studies apply their inference  
104 methodologies to functional genomics data in humans [29, 33, 36, 37]. In case human data is  
105 considered, either cell line data are used [36], the inference is restricted to a single pathway  
106 [37] or no informative priors are used for this specific context [29]. Zuo *et al.* apply prior  
107 based inference to human cancer gene expression data, however, they only use priors based  
108 on PPIs extracted from the STRING database and focus on differential expression analysis  
109 [33]. What is still missing, is, to comprehensively integrate the vast amount of functional  
110 data from large-scale databases [38–41] as prior information in human multi-omic *trans*-QTL  
111 studies and to determine the appropriate inference methods.

112 Here, we developed a novel approach for understanding the molecular mechanisms un-  
113 derlying the statistical associations of *trans*-QTL hotspots by integrating existing biological  
114 knowledge and available multi-omics data to infer regulatory networks. We derived a com-  
115 prehensive set of continuous priors from public datasets such as GTEx, the BioGrid and  
116 Roadmap Epigenomics and applied state-of-the-art network inference methods including  
117 graphical lasso [42], BDgraph [29] and iRafnet [32], and showed, that methods using data-  
118 driven priors outperform non-prior approaches for network reconstruction on simulated data.  
119 Moreover, we showed that networks inferred on real-world data using priors can be replicated  
120 more faithfully across independent datasets than networks inferred without priors. Finally,  
121 we demonstrated, that incorporating existing knowledge with multi-omics data yields novel  
122 insights into disease related cellular mechanisms when applied to real-world population co-  
123 hort data of different omics types and tissues.

## 124 Results

### 125 Trans-QTL hotspots define regulatory network candidates

126 In this study, we aimed to reconstruct regulatory networks to explain *trans* quantitative trait  
127 locus (*trans*-QTL) hotspots on a molecular level through simultaneous integration of multi-  
128 omics data [4]. *Trans*-QTL hotspots have previously been associated with disease [8, 13], and  
129 understanding their mechanisms of action can deepen our insights into regulatory pathways  
130 and, ultimately, into the disease process.

131 Our general analysis strategy is depicted in Figure 1A and consists of the following steps:  
132 1) curate QTL hotspots, 2) gather functional data and prior information, 3a+b) benchmark  
133 network inference methods in simulation and replication study to select best suited method  
134 and 4) infer and interpret networks identified in the cohort data.

135 We obtained *trans* hotspots from the methylation QTL (meQTL) discovered in whole-

136 blood in the KORA [43] and LOLIPOP [44] cohorts reported by Hawe and colleagues [10]  
137 and the expression QTL (eQTL) published by the eQTLGen consortium [7], yielding a total  
138 of 107 and 444 *trans* -loci per QTL type, respectively (Figure 1B, see Methods for details).  
139 In addition to the whole-blood derived hotspots, we curated a single *trans* -eQTL hotspot  
140 in Skeletal Muscle tissue from GTEx v8 [38, 39], which we analyzed separately.

141 For each hotspot, we aimed to identify the causal gene at the genetic locus affected by  
142 the SNP and the intermediate genes which mediate the observed *trans* associations. To  
143 this end, we collected sets of candidate genes with different roles for each locus, which  
144 we term 'locus sets' (see Methods). A locus set contains the SNP defining the hotspot,  
145 the respective *trans* associated traits (CpGs for meQTL and genes for eQTL, 'eGenes'),  
146 *cis* genes encoded near the SNP as candidate causal genes, *trans* genes (for meQTLs, genes in  
147 vicinity of the CpGs), as well as transcription factors (TFs) binding near the *trans* associated  
148 entities and PPI genes residing on the shortest path between *trans* traits and *cis* genes in  
149 a protein-protein interaction (PPI) network, as potential intermediate genes. *Cis* genes  
150 form potential candidate regulator genes of the locus, and the inclusion of the PPI and TF  
151 binding information allows us to bridge the inter-chromosomal gap between the SNP and  
152 the *trans* CpG sites/*trans* eGenes. An overview of entities collected over all loci for both  
153 QTL types is given in Figure 1C.

154 One main aspect of this work is the use of any form of biological prior information,  
155 including continuous scores, to guide network inference. We hence collect prior information  
156 for all possible edges between entities contained in locus sets in addition to the functional  
157 data (Figure 1). In total, four distinct types of edges are annotated with prior information:  
158 *SNP-Gene*, *Gene-Gene*, *TF-CpG/TF-Gene* and *CpG-Gene* edges. All prior information is  
159 generated from matched, public data independent of the data used during network inference  
160 (see Methods for details).

161 Figure 1D indicates the total number of edges annotated with prior information over

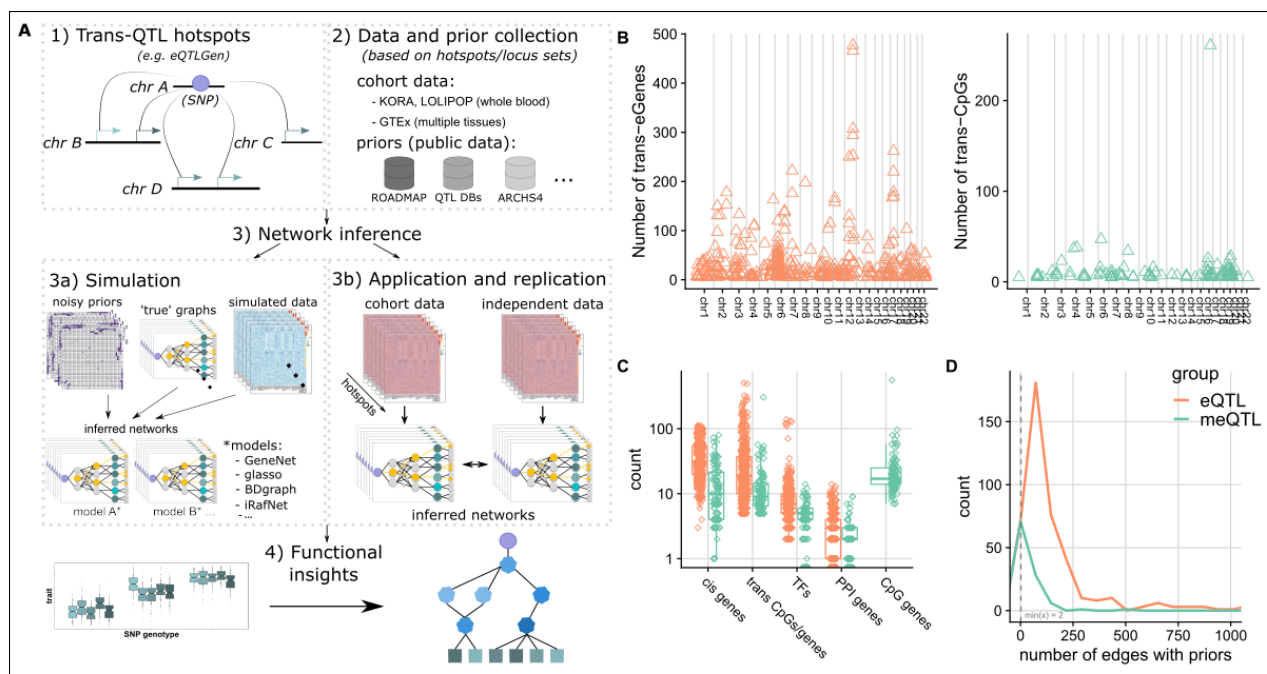


Figure 1: Project overview. Panel **A**) shows a graphical abstract of the analyses performed in this project. Panel **B**) provides a global view on the collected eQTL (orange) and meQTL (green) hotspots. The x-axis indicates ordered chromosomal positions for *trans* eGenes and CpG sites, respectively. Panel **C**) shows the total number of different genomic entities gathered over all hotspots during locus set creation (log scale). Panel **D**) depicts density plots of the number of possible network edges with available prior information (x-axis) over all hotspots, zoomed in to area between 0 and 1000. Same color coding is used in panels **B-D**.

162 all hotspots. For meQTL and eQTL, a minimum of 2 and 3 edges per hotspot show prior  
 163 evidence, respectively, and most hotspots get only relatively few priors compared to the total  
 164 number of possible edges (median 26 and 94, respectively). However, in both cases several  
 165 networks collect priors for over 100 edges (8 and 209 loci with  $\geq 100$  priors for meQTL and  
 166 eQTL). As expected, the total number of edges with prior information per locus correlates  
 167 with the total number of possible edges in the respective loci, however, the fraction of all  
 168 possible edges annotated with prior information decreases (Additional File 1, Figure S2).

## 169 Benchmark of network inference methods

### 170 Simulation study shows benefit of data-driven priors

171 Numerous methods for regulatory network inference have been proposed (e.g. [42, 45, 46], see  
172 also [4]), and, therefore, before investigating individual hotspots in detail we sought to select  
173 the method best suited for this study (see Figure 1A step 3). To this end, we performed an  
174 extensive simulation study (Figure 1A step 3a) to evaluate the performance of five distinct  
175 methodologies (see Table 1 for a method overview) in reconstructing ground truth graphs  
176 from simulated data and prior information. Simulated data were matched with the observed  
177 QTL-hotspots by preserving the sample size and the total number of input nodes and 100  
178 simulations were performed for each hotspot. We evaluated the impact of priors for different  
179 sample sizes by sub-sampling the simulated data and using the full prior matrix. To assess  
180 the impact of noise in priors, we inferred networks separately from prior information with  
181 varying degrees of noise (up to 100%, see Methods for details) for the complete data.

name	version	repository	attribute	reference
<i>BDgraph</i>	2.61	CRAN	MCMC	Mohammadi and Wit (2015) [29]
<i>gLASSO</i>	1.11	CRAN	Graphical lasso	Friedman <i>et al.</i> (2008) [42]
<i>GENIE3</i>	1.2.1	bioconductor	Random forests	Huynh-Thu <i>et al.</i> (2010) [46]
<i>GeneNet</i>	1.2.13	CRAN	Shrinkage/ FDR	Opgen-Rhein <i>et al.</i> (2007) [45]
<i>iRafNet</i> *	1.1-2	CRAN	Random forests	Petralia <i>et al.</i> (2015) [32]

Table 1: Overview of the network inference packages used in the simulation study.

\* *adjusted to make use of parallel processing, see Methods*

182 We gauge the relative gain in performance attributable to prior information for both  
183 *gLASSO* and *BDgraph* by always training two distinct models, one utilizing the provided  
184 priors ( $gLASSO_P$ ,  $BDgraph_P$ ) and one without priors ( $gLASSO$ ,  $BDgraph$ ). The  
185 implementation of *iRafNet* always requires a prior matrix, whereas both *GeneNet* and



186 *GENIE3* cannot utilize prior information and hence were trained only with the simulated  
187 data. We utilize Matthews Correlation Coefficient (MCC) [47] as a balanced performance  
188 measure to compare inferred networks to the respective ground truth (see also [29]). Fig-  
189 ures 2A and 2B show the results for the simulation study for all methods (see also Additional  
190 File 1, Tables S2, S3, S4 and S5). Overall, both *gLASSO<sub>P</sub>* and *BDgraph<sub>P</sub>* exhibit improved  
191 performance with relatively low standard deviation in terms of MCC as compared to their  
192 non-prior counterparts, both for low and high sample size settings. The performance of all  
193 other methods is affected by low sample sizes, with *BDgraph* showing slightly better perfor-  
194 mance than all other methods. Moreover, both *gLASSO<sub>P</sub>* and *BDgraph<sub>P</sub>* outperform all  
195 other methods as long as the prior noise does not exceed 10% (*gLASSO<sub>P</sub>*) and 30% of incor-  
196 rect edges in the prior graph, in which case *BDgraph* achieves the highest median MCC over  
197 all methods. *GeneNet* performs well in all simulations, whereas *GENIE3*, *gLASSO* and  
198 *iRafNet* show about average performance with *iRafNet* achieving worst results overall.  
199 In addition to the curated prior matrices, we also generated a prior matrix reflecting the  
200 sparsity of the true graph (column 'rbinom' in Figure 2B and Additional File 1, Tables S2  
201 and S3, see also Methods), and our results indicate, that information about sparsity of the  
202 underlying network already improves network inference performance. Finally, prior based  
203 methods, and specifically *BDgraph<sub>P</sub>*, outperform non-prior methods in the task of identify-  
204 ing the correct *cis*-gene by recovering associations between the discrete SNP and continuous  
205 gene expression data types (Additional File 1, Figure S3), when using independent eQTL  
206 data as prior.

## 207 **Inferred networks replicate in independent datasets**

208 In addition to the simulation study, we evaluated the methods on real world data from  
209 two large population cohorts: the KORA (Cooperative Health Research in the Region of  
210 Augsburg) and LOLIPOP (London Life Sciences Population) cohorts (see Figure 1A2 and

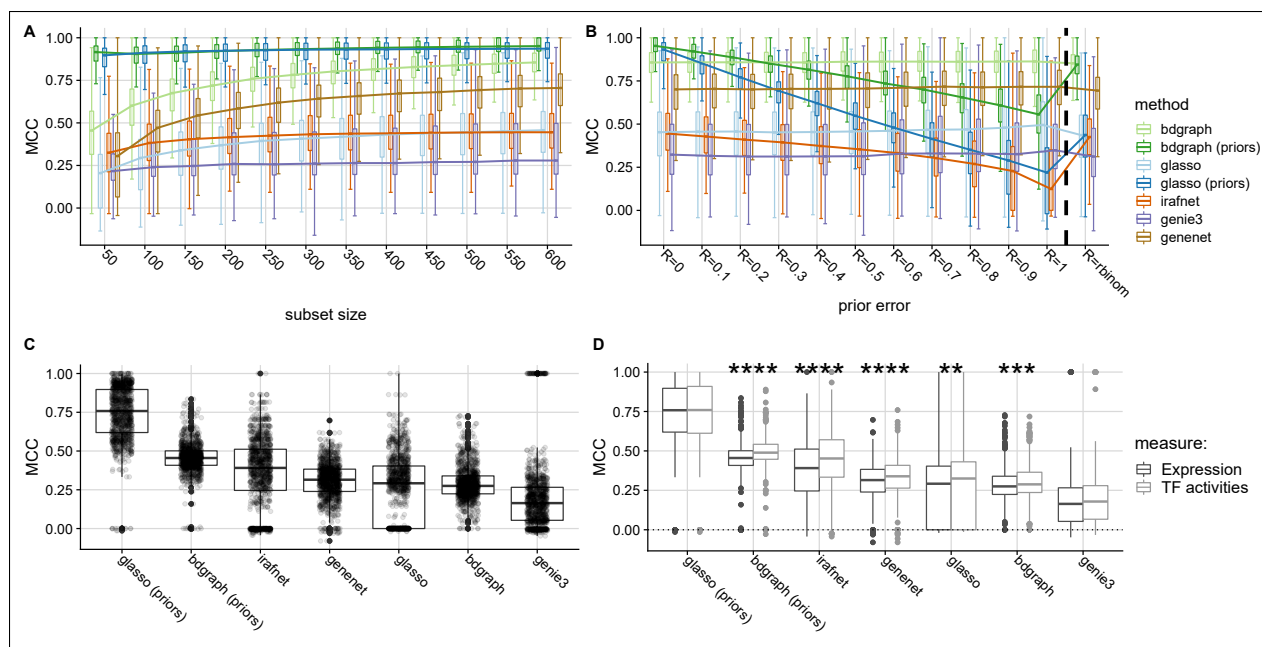


Figure 2: Method comparison results. **(A)** Results of simulation study: y-axis shows the Matthews correlation coefficient (MCC) as compared to the simulated ground truth, x-axis indicates increasing sample size from left to right, colors indicate different inference methods. **(B)** Similar to (A), but x-axis indicates increasing noise in the prior matrix from left to right. Group ('rbinom') indicates uniform prior set to reflect degree distribution of true graph. **(C)** shows MCC (y-axis) between networks inferred on KORA and LOLIPOP data for same locus for all methods (x-axis). **(D)** contrasts MCC across cohorts using TF expression (dark gray) versus using substituted TFAs (light gray). Boxplots show medians (horizontal line) and first and third quartiles (lower/upper box borders). Whiskers show  $1.5 * IQR$  (inter-quartile range); for **(B)**, dots depict individual results and for **(C)**, stars indicate significant difference between expression/TFA results for each method (Wilcoxon test, \*\*:  $P \leq 0.01$ , \*\*\*:  $P \leq 0.001$ , \*\*\*\*:  $P \leq 0.0001$ )

211 Methods). Data from both cohorts were generated from whole-blood samples and contain  
 212 imputed genotypes as well as microarray measurements of gene expression and DNA methy-  
 213 lation for a total of 683 (KORA) and 612 (LOLIPOP) samples. Since for these data no  
 214 ground truth is available, we evaluate robustness of the networks inferred by the individual  
 215 methods via cross cohort replication. For each hotspot, we collect data for all genes, CpGs  
 216 and the SNP in the locus set for KORA and LOLIPOP and separately inferred networks  
 217 in both cohorts for all models. Obtained networks were then compared between cohorts

218 using MCC to get a quantitative estimate of how robust the network inference is across  
219 different datasets for the same hotspot, yielding scores for KORA versus LOLIPOP and  
220 vice versa (i.e. one network functioning as the reference). Results of this analysis are shown  
221 in Figure 2C. With respect to MCC, models supplied with prior information ( $gLASSO_P$  ,  
222  $BDgraph_P$  and  $iRafNet$  ) show the best performance, with  $gLASSO_P$  coming up as the  
223 most robust method, followed by  $BDgraph_P$  and  $iRafNet$  . Noticeably, of the top methods  
224  $BDgraph_P$  shows much less variance compared to  $gLASSO_P$  and  $iRafNet$  . Ignoring prior  
225 information lead to a drop in performance for both  $gLASSO$  and  $BDgraph$  , which leads to  
226  $GeneNet$  outperforming both methods. Finally,  $GENIE3$  shows worst performance in this  
227 setting.

## 228 **Estimated transcription factor activities as a proxy to TF activation**

229 Transcription factor activities (TFAs) estimated from transcription factor binding sites (TFBS)  
230 and gene expression data have been suggested as an alternative to using TF gene expres-  
231 sion in inference tasks [48], since a transcription factor’s expression level alone might not  
232 reflect the actual activity of a TF (driven for instance by its phosphorylation state). To  
233 evaluate, whether TFAs could improve our inference, we estimated TFAs for all TFs based  
234 on their expression and ChIP-seq derived TFBS from ReMap [49] and ENCODE [50, 51]  
235 (see Methods for details). We applied the same cross cohort replication strategy as above  
236 and compared MCCs from the TFA based analysis to the previous results using a one-sided  
237 Wilcoxon test. Figure 2D shows the results of TFA (light gray boxes) versus gene expres-  
238 sion (dark gray boxes) based analysis in terms of MCC for all available hotspots. For all  
239 models but  $gLASSO_P$  and  $GENIE3$  , TFAs yield a significantly higher MCC (Wilcoxon  
240 test  $P < 0.01$ ) as compared to using the pure expression data (see also Additional File 1,  
241 Table S6).

242 According to the results presented above, detailed investigation of real world data was

243 focused on networks obtained from  $gLASSO_P$  and  $BDgraph_P$  and TF expression was sub-  
244 stituted by TFA estimates for all subsequent analyses.

## 245 Replication of previous findings by simultaneous data integration

246 Before seeking new mechanistic insights and generating novel hypotheses from *trans*-QTL  
247 hotspots, we first checked whether our approach can replicate previous findings. Hawe  
248 *et al.* [10] inferred gene regulatory networks from *trans*-meQTL hotspots using a two-  
249 step approach involving 1) a random walk on a PPI and ChIP-seq based networks and 2)  
250 subsequent local correlation analysis. In contrast, our approach simultaneously integrates  
251 all functional data, relying on PPI and ChIP-seq information as prior knowledge, thereby  
252 avoiding the need for post-hoc correlation testing of e.g. SNP-gene and CpG-gene edges. For  
253 the comparison, we extracted three of their hotspot networks and evaluated the overlap with  
254 the networks inferred in this study.

locus	num. nodes	num. edges	common edges	MCC
rs9859077	99 (89)	447 (287)	141	0.52
rs730775	58 (49)	98 (67)	48	0.69
rs7783715	25 (17)	24 (23)	5	0.65

Table 2: Comparison of the networks inferred in this study to the networks extracted from [10]. Numbers in bracket indicate statistics for the networks from the original publication.

255 Table 2 shows the results of this comparison. Overall, the comparisons indicate rela-  
256 tively strong concordance between the two approaches with MCCs of 0.515, 0.689 and 0.65.  
257 Moreover, for all three networks, our simultaneous inference approach yielded more edges  
258 and nodes than the two-step approach (56%, 46% and 4% novel edges and 11%, 19%, 47%  
259 additional nodes for rs9859077, rs730775 and rs7783715, respectively), which might have  
260 been missed by the two-step approach, as it relies on known PPI and ChIP-seq information.

261 Figure 3 contrasts the two networks obtained for the *rs730775* hotspot using 1) the two-  
262 step approach by Hawe *et al.* [10] and 2) the network inferred in this study using  $gLASSO_P$ ,

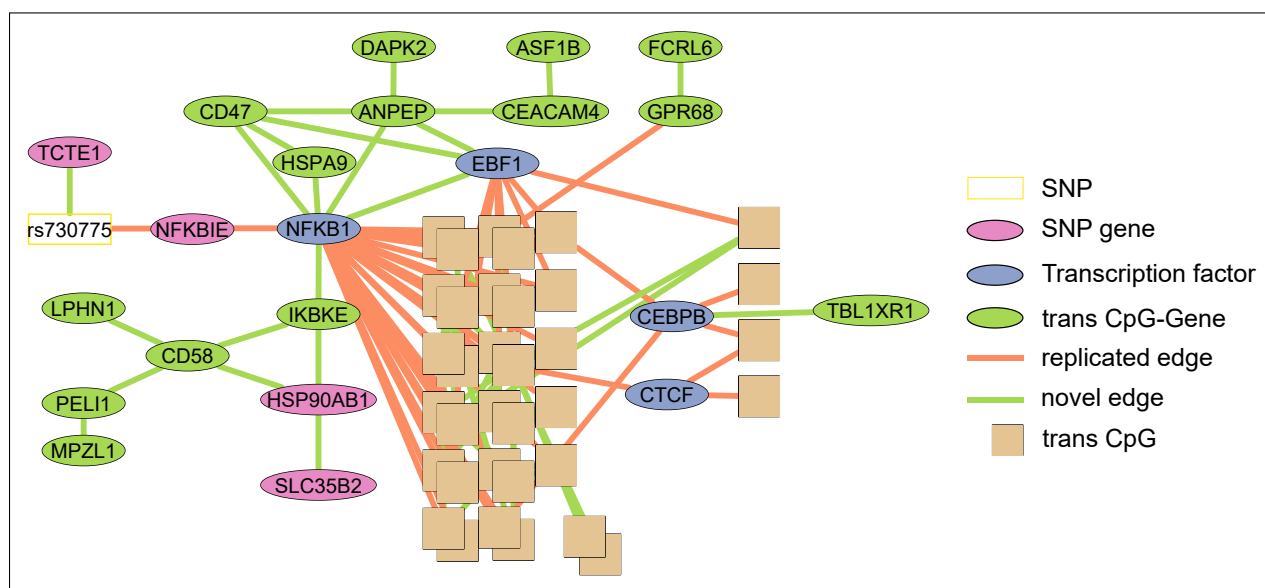


Figure 3: Comparison of the random walk based network reported in [10] and the network inferred from functional omics data in this study for the rs730775 locus. Shown is the complete network constructed from the omics data, edge color indicates replication/novelty. Orange edges: replicated with respect to the random walk network. Green edges: novel in our network. White box: SNP; pink nodes: SNP-genes; blue nodes: TFs; brown boxes: CpGs; green nodes: CpG-genes.

263 orange edges showing replicated and green edges indicating novel edges. In Hawe *et al.*  
264 [10], the authors described a regulatory network involving the *rs730775* SNP connected  
265 via *NFKBIE* to *NFKB1* which connects to the trans-CpG sites. This main pathway is also  
266 discovered in our approach (i.e.  $rs730775 \leftrightarrow NFKBIE \leftrightarrow NFKB1 \leftrightarrow CpG\ sites$ ), in addition  
267 to some of the initially reported TFs (blue nodes), of which *NFKB1* is connected to most  
268 of the *trans* CpGs (82%, 29 out of 35) as was the case in the original network. However,  
269 we also identify patterns of CpG genes (green nodes) connected to the TFs, which were not  
270 previously identified. Overall, the integrated approach using prior information leads to high  
271 replication of previous networks including novel connections leading to potential new insights  
272 in target gene regulation.

## 273 **A trans regulatory network for a schizophrenia susceptibility locus**

274 In order to demonstrate the effectiveness of our approach in getting mechanistic insights  
275 from *trans* -QTL associations, we inferred networks for all meQTL [10] and eQTL [7]  
276 hotspots using whole blood data from the KORA and LOLIPOP cohorts using the prior  
277 based *gLASSO<sub>P</sub>* and *BDgraph<sub>P</sub>* models (see Methods, all networks are listed in Additional  
278 File 2, Table S3). Based on the GWAS catalog (v1.0.2, [52]), graph properties and a cus-  
279 tom graph score (see Methods), we prioritized a *trans* acting locus that has previously been  
280 associated with schizophrenia (SCZ).

281 The network involves the *trans* -eQTL locus around the *rs9469210* (alias *rs9274623*<sup>1</sup>)  
282 SNP in the Human Leukocyte Antigen (HLA) region on chromosome 6 shown in Figure 4A.

283 *rs9274623* has been associated with SCZ [54] and is a *cis* -eQTL for all three of its  
284 directly connected SNP-genes, *PBX2*, *RNF5* and *HLA-DQA1* in the eQTLGen study. *RNF5*  
285 showed differential expression for SCZ cases vs controls in addition to its expression being  
286 associated with an additional independent SCZ susceptibility SNP (*rs3132947*,  $R^2 = 0.14$

---

<sup>1</sup>according to SNIIPA: <https://snipa.helmholtz-muenchen.de/snipa3/>, [53]

287 in 1000 genomes Europeans<sup>2</sup>) located in the HLA locus [55]. Interestingly, *PBX2* has been  
288 associated with a SCZ related phenotype in a pharmacogenetics study (clozapine-induced  
289 agranulocytosis) [56, 57] and shows direct binding evidence to the *SPI1* promoter region  
290 (ReMap TFBS [49]). The transcription factor *SPI1* (*PU.1*) is linked to Alzheimer's Disease  
291 likely by impacting neuroinflammatory response [58] and was found to interact with its  
292 network neighbor, *RUNX1*, in modulating gene expression [59]. Moreover, *RUNX1* has been  
293 implicated in rheumatoid arthritis, a disease negatively associated with SCZ and which  
294 hence might share susceptibility genes with SCZ [60]. Interestingly, several genes encoded  
295 in the HLA locus, which has been implicated in SCZ and other psychiatric and neurological  
296 disorders [61–64], were picked up by our inference downstream of *SPI1* and *RUNX1*. *TCF12*  
297 is a paralog of *TCF4* and *TCF3* which are known E-box transcription factors and are  
298 expressed in multiple brain regions [65]. *TCF4* loss-of-function mutations are the cause  
299 of Pitt-Hopkins syndrome (a syndrome causing mental retardation and behavioral changes  
300 amongst other symptoms) [66] and regulatory SNPs relating to *TCF4* have been associated  
301 with SCZ [67, 68]. The *NFKB1* pathway has been recognized as an important regulatory and  
302 developmental factor of neural processes and was found to be dysregulated in patients with  
303 SCZ [69]. Finally, 9 of the 40 discovered *trans*-eGenes of the locus are connected to the SNP  
304 via the selected TFs. Of these, *SH3BGRL3* [70] has already been linked to SCZ and *PSEN1*  
305 [71], *B9D2* [72], *CXCR5* [73] as well as *DNAJB2* [74] were implicated in other neurological  
306 disorders. In addition, the *trans* eGene *RNF114* has previously been shown to play a role  
307 in the *NFKB1* pathway [75]. A formal colocalization analysis using fastENLOC [76] showed  
308 evidence of a common causal variant underlying the SCZ GWAS signal [77] and each of the  
309 eQTLGen *trans*-eQTL of *PSEN1*, *DNAJB2* and *CD6* (SNP-level colocalization probability  
310 of 0.92, 0.87 and 0.42, respectively; see Methods and Additional File 1, Figure S4).

311 Our approach highlighted a potential regulatory pathway involving diverse genes related

---

<sup>2</sup><https://ldlink.nci.nih.gov/?tab=ldmatrix>

312 to SCZ and other neurological disorders. While some of the genes were not previously  
 313 reported in this specific disease context (e.g. *CD6*, *BRD2*, *DEF8*), their association to this  
 314 network indicates a potential role in SCZ pathogenesis and additional colocalization analysis  
 315 hints at a potential causal relationship between these genes and SCZ.

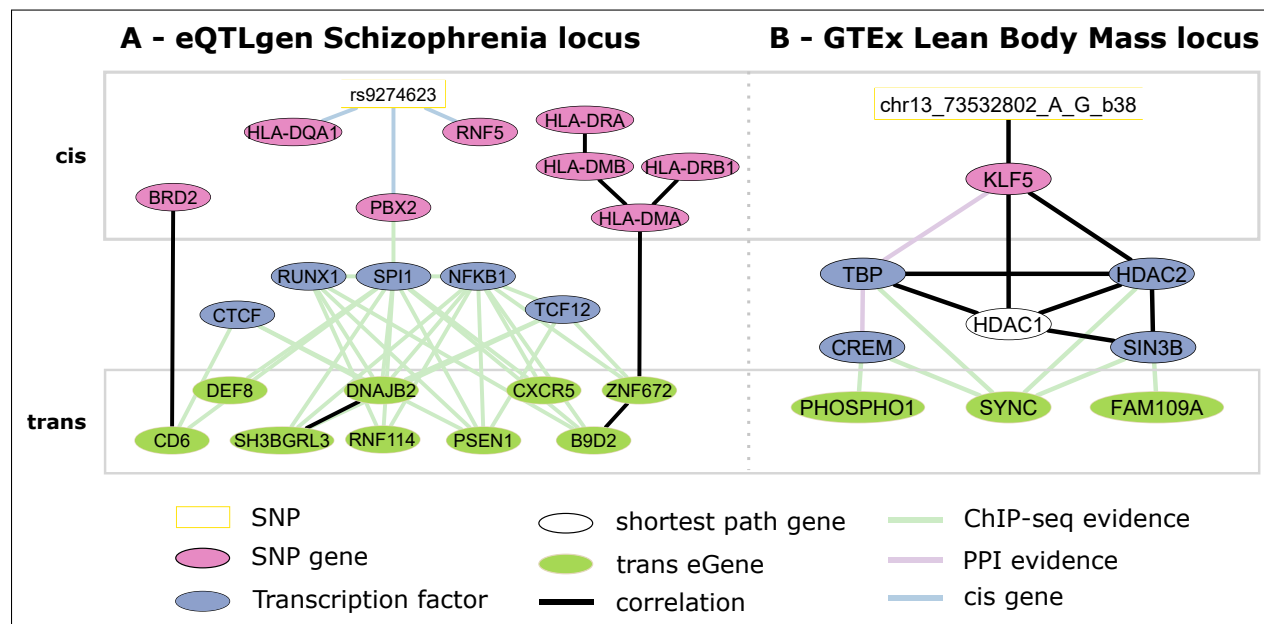


Figure 4: Inferred networks for the schizophrenia susceptibility locus rs9274623 obtained from eQTLgen (A) and the rs9318186 locus obtained from GTEx (B). The white boxes indicate sentinel SNPs, pink ovals indicate SNP-Genes, blue ovals transcription factors and white ones shortest path derived genes. Light green ovals represent genes trans-associated to the SNP. Black edges were inferred during network inference. In addition to being inferred, colored edges indicate ChIP-seq protein-DNA binding evidence (green), protein-protein interaction in the BioGrid (purple) and whether or not a gene is encoded in *cis* of the linked entity (blue).

## 316 Application to GTEx Skeletal Muscle tissue

317 All above analyses were focused on whole-blood data, however, the proposed strategy can  
 318 be applied to data from any biological context. To demonstrate this, we investigated the  
 319 recently published *trans* -eQTLs from the GTEx v8 release [38, 78]<sup>3</sup>. We identified a single

<sup>3</sup><https://www.gtexportal.org/>



320 LD block in Skeletal Muscle tissue, which is a *trans* -eQTL hotspot (see Methods), and  
321 for which we inferred regulatory networks. Since we can't use the same priors, which were  
322 initially derived from GTEx, to analyze the same data set, we set out to curate muscle tissue  
323 specific priors from independent datasets. We utilized muscle eQTL from Scott *et al.* (2016)  
324 [79] and gene expression data curated from the ARCHS<sup>4</sup> [41] database and generated tissue  
325 specific TFBS using factorNet [80] on DNase-seq data obtained from ENCODE [50, 51]<sup>4</sup> (see  
326 Methods for details). The resulting network for the *gLASSOP* model is shown in Figure 4B.

327 The genetic variant rs9318186 is a *cis* -eQTL of *KLF5* in GTEx v8 Skeletal Muscle  
328 ( $P = 6.1 \times 10^{-37}$ ) and a proxy of it ( $R^2 = 0.88$ ) has been associated with *Lean Body Mass*  
329 (LBM). *KLF5* itself, too, has been associated with LBM in a transcriptome-wide association  
330 study integrating GWAS results with gene expression [81] and with lipid metabolism in *KLF5*  
331 knockout mice [82]. In addition, several other genes in the network have been associated with  
332 related phenotypes: Both *HDAC1* and *HDAC2* have been found to control skeletal muscle  
333 homeostasis in mice [83], work together with *SIN3B* in the SIN3 core complex to regulate  
334 gene expression and are involved in muscle development [84]. TATA binding protein (*TBP*) is  
335 a well known transcription factor and important for the transcriptional regulation of many  
336 eukaryotic genes [85]. The *trans* -eGene *SYNC* was found to interact with dystrobrevin  
337 (*DMD* gene) in order to maintain muscle function (during contraction) in mice as well as  
338 being associated with neuromuscular disease [86, 87]. In addition, in Seim *et al.* (2018)  
339 [88], the authors investigated the relationship between obesity and cancer subtypes and  
340 found, that both *PHETA1/FAM109A* expression are associated to Body-Mass-Index (BMI)  
341 in esophageal carcinoma in data from The Cancer Genome Atlas (TCGA). *PHOSPHO1* has  
342 been found to be involved in metabolism, specifically in energy homeostasis [89], and has also  
343 been associated via DNA methylation with BMI [90, 91] and with HDL levels, which have  
344 been negatively associated with LBM [92]. Dayeh *et al.* (2016) [93] further showed decreased

---

<sup>4</sup><https://www.encodeproject.org/>

345 DNA methylation at the *PHOSPHO1* locus in skeletal muscle of diabetic vs. non-diabetic  
346 samples. The remaining gene in the network (*CREM*) has not yet been described in the  
347 broader context of LBM, but a GWAS meta-analysis executed by Wang *et al.* (2014) [94]  
348 hinted at association of a *CREM* SNP (rs1531550,  $P = 1.88 \times 10^{-6}$ ) with elite sprinter status.  
349 These results suggest, that *KLF5* may exert its specific functions through transcriptional  
350 regulation via the SIN3 core complex including *TBP*, with a potential involvement of *CREM*,  
351 of the *trans* -eGenes *PHOSPHO1*, *SYNC* and *PHETA1/FAM109A*.

## 352 Discussion

353 In this study, we introduced a Bayesian framework for the inference of undirected regulatory  
354 networks underlying molecular *trans* -QTL hotspots across multi-omics data types using  
355 existing prior knowledge. We compiled a comprehensive set of context specific network edge  
356 priors from diverse biological databases and applied these together with multi-omics data in  
357 different settings. These settings include an extensive simulation study to benchmark state-  
358 of-the-art inference methods as well as application to two large population cohorts, which  
359 we use for a replication analysis on the one hand and to generate novel hypotheses about  
360 molecular disease mechanisms on the other hand. Moreover, by applying our approach a  
361 GTEx Skeletal Muscle eQTL hotspot, we showed, that our strategy can be applied to data  
362 sets from other tissues, generated with different technologies.

363 Benchmarking is important for selecting the best possible methods for specific tasks and  
364 we hence followed recently published guidelines [95] to perform benchmarking of state-of-  
365 the-art network inference methods in 1) a simulation study and 2) a replication analysis.  
366 Results from both analyses were then used to select the methods best suited for network  
367 inference based on functional multi-omics data from QTL hotspots using prior information.

368 By inferring networks in over 10,000 simulated data sets, which reflect the distribution of

369 network parameters obtained from real-world data, we showed, that methods utilizing prior  
370 information outperform methods without any prior information in recovering a simulated  
371 ground truth, similar to what has been found e.g. in [27, 28, 36]. We further observed  
372 that, as expected, too much noise in the prior information significantly reduces method  
373 performance. However, only by increasing the noise level, i.e. the percentage of incorrect  
374 prior edges, to above 30% decreases the performance for BDgraph below the performance  
375 of its non-prior counterpart, indicating that low levels of noise in edge priors still improve  
376 network inference, results which are in line with e.g. Wang *et al.* (2013) [30], who used  
377 a modified graphical lasso approach, Christley *et al.* (2009) [28], who used an regularized  
378 ODE model and Greenfield *et al.* (2013) [27], who used a Bayesian regression framework.  
379 We further find, that, both for the prior and non-prior case, the Markov-Chain-Monte-Carlo  
380 based  $BDgraph_P$  method outperforms respective other methods. However, both the copula  
381 approach based BDgraph and the  $gLASSO_P$  outperform other methods in recovering mixed  
382 edges between discrete SNP allele dosage and continuous gene expression levels, although  
383 the tree based methods should be able to incorporate mixed data. While  $BDgraph_P$  shows  
384 overall better performance than  $gLASSO_P$ , the graphical lasso exhibits much lower run  
385 time which can be an important practical consideration. Our results hence highlight the  
386 strong value of using prior information for multi-omics based network reconstruction, and  
387 slightly favor BDgraph over the graphical lasso for this kind of inference.

388 We confirmed the results of the simulation study by extended benchmarking of inference  
389 methods in a cross cohort replication analysis on two large multi-omics data sets. Prior  
390 based methods showed overall best replication across different cohorts as compared to non-  
391 prior methods. In the real-world setting, however, *iRafNet* performed similarly well as the  
392 other two prior methods in contrast to the simulation study and all prior based methods  
393 outperform non-prior methods. The good replication of prior based methods across different  
394 cohorts shows, that curated priors help to obtain more stable and confident results as com-

395 pared to using functional data alone. Together with the simulation, these results provide a  
396 comprehensive benchmark of established network inference methods and suggest, that priors  
397 should be integrated in network inference tasks wherever possible.

398 Based on the results from the replication and simulation study, we choose the two best  
399 (prior based) methods  $BDgraph_P$  and  $gLASSO_P$  for detailed investigation of networks  
400 obtained from real-world cohort data. Using our integrative approach, we were able to  
401 reproduce and expand upon previous results from a step-wise network analysis approach  
402 presented in [10]. Of three of the locus networks described in their study, we reconstructed  
403 most of the edges and found additional edges, allowing more mechanistic interpretations for  
404 the function of specific transcription factors in relation to DNA methylation. One reason for  
405 finding additional edges is, that these could not be detected by the previous approach, since  
406 the authors focused on using established PPI and protein-DNA interactions and did not test  
407 all possible edges in the functional data. In contrast, our integrated approach considers all  
408 edges regardless of available prior evidence and associations will emerge, if the signal in the  
409 functional data alone or in addition to the prior evidence is strong enough.

410 Next, we utilized the two top performing methods ( $BDgraph_P$  and  $gLASSO_P$ ) to infer  
411 networks from *trans* -eQTL hotspots and found, that our strategy can be used to recover  
412 known biology on the one hand and generate novel hypotheses about the molecular basis  
413 of diseases on the other hand. For a schizophrenia (SCZ) susceptibility locus, we identified  
414 several known SCZ (e.g. *RNF5*, *HLA genes* [55, 61]) and related (e.g. *PBX2* [56, 57]) genes  
415 in the inferred locus network. Caution is needed for the interpretation of the candidates  
416 based on *cis* -eQTL, because of the haplotype structure of the HLA locus. However, our  
417 candidate *PBX2* is defined by its connections in the network to the *trans* genes and, there-  
418 fore, independent of the *cis* eQTL. Expanding upon similar previous observations based on  
419 *trans* eQTL [7], the integrated network analysis including associated *trans* genes prioritizes  
420 *PBX2*, which was not possible using *cis* -eQTL alone. It was previously hypothesized, that

421 *RUNX1* is involved in SCZ due to a negative association of SCZ with rheumatoid arthritis  
422 [60]. Our network corroborates this hypothesis and further allows for generating novel hy-  
423 potheses about the involvement of other genes (e.g. *BRD2*, *DEF8* and *RNF114*), which could  
424 potentially play a role in schizophrenia. Moreover, we further substantiated these results by  
425 a formal colocalization analysis of the *trans* -eQTL and schizophrenia GWAS [77] signals of  
426 the *trans* genes linked in the network, which revealed strong evidence for colocalization of  
427 the underlying genetic variants of the disease and molecular traits. As this locus was derived  
428 from whole-blood data, interpretation is not straight forward for SCZ. Ideally, this analysis  
429 can be followed up in data derived from brain tissue to corroborate findings.

430 To show, that our approach can be applied across different omics types and data sets,  
431 we analyzed a Skeletal Muscle *trans* -eQTL hotspot from GTEx associated with Lean Body  
432 Mass. We recovered known genes involved in lipid metabolism (*KLF5* [81, 82]) as well  
433 as muscle development and controlling skeletal muscle homeostasis (e.g. *HDAC1*, *HDAC2*,  
434 [83]) and maintaining muscle function (*SYNC* [87]). This shows, that the genes linked in  
435 the inferred network are overall coherent with the observed phenotype association at this  
436 *trans* -acting locus. Moreover, *HDAC1*, *HDAC2* and *SIN3B* have been described to interact  
437 together during muscle development [84], and, although these results were described in mice,  
438 our results suggest that these genes could exhibit a similar function in human. In addition,  
439 we observed an association between *CREM* and *SYNC* in our network, which led us to  
440 hypothesize, that *CREM* might also be involved in maintaining muscle function and Lean  
441 Body Mass, although it has not been previously linked to these phenotypes. However,  
442 additional experimental validation needs to be performed in order to corroborate findings of  
443 these computational analyses.

444 Several practical considerations arise from our findings: First, by investigating the effect  
445 of increasing amounts of noise in the prior information in our simulation study, we showed,  
446 that some caution needs to be applied when curating continuous prior information from

447 public biological data to keep noise levels low. Therefore, although  $gLASSO_P$  and especially  
448  $BDgraph_P$  seem to be robust to low to moderate levels of noise, one might consider using  
449 only experimentally validated protein-protein interactions or high quality gene expression  
450 data to generate priors. Next, the definition of hotspot locus sets and priors in this study  
451 mitigates the  $N \ll P$  problem. This has been a problem sought to be alleviated using  
452 specialized approaches in previous applications [4]. Using our approach, the total number  
453 of entities (variables) going into the network inference typically does not exceed the total  
454 number of available samples in our data sets, and we showed in a simulation study, that priors  
455 improve inference also in low sample size settings. Overall, the benefit of the locus sets comes  
456 with the risk of missing certain genes needed to fully describe the *trans* effects. For instance,  
457 we reason that most relevant genes lie on the shortest path between *cis* and *trans* entities in  
458 the PPI network and hence only included those shortest path genes. However, our strategy  
459 of curating a stringent set of relevant transcription factors as well as including genes showing  
460 protein-protein interactions and all the genes in the vicinity of the hotspot SNP, should enable  
461 most key regulator genes to enter the inference process and yields parsimonious and easily  
462 interpretable results. In addition, methods have been developed to handle mixed data types,  
463 such as e.g. genotypes and gene expression.  $BDgraph$ , which uses a copula based approach  
464 to transform non-normal data, showed better performance in recovering associations between  
465 discrete and continuous data types as compared to  $gLASSO$  and the tree based methods, and  
466 hence should be preferred for applications on mixed data, especially when prior information  
467 is available. Finally, while we could use transcription factor binding sites (TFBS) in blood  
468 related cell-lines to analyze whole-blood cohort data, context (e.g. tissue) specific TFBS  
469 are not yet available for a large number of transcription factors, which potentially limits  
470 this approach to fewer applications. However, novel developments to predict TFBS from  
471 context specific open chromatin information (e.g. *factorNet* [80]) can help in carrying this  
472 strategy to more contexts. As an example, we utilized TFBS predicted using *factorNet* based

473 on ENCODE [50, 51] DNase-seq data for analyzing a GTEx Skeletal Muscle *trans* eQTL  
474 locus.

## 475 Conclusion

476 This study describes a novel strategy for using comprehensive edge-wise priors from biological  
477 data to improve network inference for *trans*-QTL hotspots from human population scale  
478 multi-omics data. This facilitates the investigation of their underlying regulatory networks  
479 and enables the generation of novel mechanistic hypotheses for disease associated genetic  
480 loci. Moreover, we report a rigorous benchmark of state-of-the-art network inference methods  
481 for this task both in simulated and real-world data, and highlight the benefit of including  
482 biological prior information to guide network inference.

## 483 Methods

### 484 Cohort data processing

Methylation data were measured using the Infinium Human Methylation 450K BeadChip in both the KORA and the LOLIPOP cohort and methylation beta values obtained as described previously [43, 44]. Quantile normalized methylation beta values were adjusted for Houseman blood cell-type proportion estimates and the first 20 principal components calculated on the array control probes by using residuals of the following linear model:

$$methylation\ \beta \sim 1 + CD4T + CD8T + NK + BCell + Mono + PC1 + \dots + PC20$$

485 For expression data, the Illumina HumanHT-12 v3 and Illumina HumanHT-12 v4 expres-  
486 sion BeadChips were used in KORA and LOLIPOP, respectively, and processed as described

487 previously [10, 96]. Only probes common to both arrays were selected for analysis. Expres-  
488 sion data were adjusted for potential confounders by regressing log2 transformed expression  
489 values against age, sex, RNA integrity number (RIN) as well as RNA amplification plate  
490 (KORA) / RNA conversion batch (LOLIPOP) (batch1) and sample storage time (KORA)  
491 / RNA extraction batch (LOLIPOP) (batch2) and obtaining the residuals from the linear  
492 model:

$$expression \sim age + sex + RIN + batch1 + batch2$$

493 Additional details on the cohort data and design are presented in [43, 96, 97] (KORA)  
494 and [44, 98] (LOLIPOP).

495 For the inference of the GTEx Skeletal Muscle related network, we used GTEx v8 Skeletal  
496 Muscle data [78]. Potential confounders including first 5 genotype PCs, 60 expression PEER  
497 factors and measured covariates 'WGS sequencing platform' (HiSeq 2000 or HiSeq X), 'WGS  
498 library construction protocol' (PCR-based or PCR-free) and donor sex, were removed from  
499 expression data prior to analysis. Processing has been performed as previously described  
500 and details can be found elsewhere [78].

## 501 Hotspot extraction and construction of locus sets

502 We extract sub-sets of genomic entities (SNPs, CpGs and genes) on which we perform  
503 network inference based on the *trans* -meQTL reported by [10] (Supplementary Table 9 of  
504 their study) and eQTLGen *trans* -eQTL [7]<sup>5</sup>. For GTEx, we obtained current (GTEx v8)  
505 tissue specific *trans* -eQTL from <https://www.gtexportal.org/home/datasets><sup>6</sup>.

506

507 **Hotspot extraction.** The list of *trans* -meQTL results obtained from [10] was already

---

<sup>5</sup>obtained from <https://eqtlgen.org/trans-eqtls.html>

<sup>6</sup>file GTEx\_Analysis\_v8\_trans\_eGenes\_fdr05.txt



508 pruned for independent genetic loci and was used as provided in the paper supplement. To  
509 remove redundant highly correlated genetic loci, we pruned the eQTLGen *trans* -eQTL by  
510 selecting the eQTLs with 1) the highest minor allele frequency and 2) the largest number  
511 of *trans* genes for each LD cluster (1Mbp window,  $R^2 > 0.2$ ). For GTEx, we merged eQTL  
512 by combining SNPs with  $R^2 > 0.2$  and distance  $< 1$ Mbp to independent genetic loci and  
513 kept all *trans* -eGenes (eGenes: genes associated with eQTL genotype) of the individual  
514 SNPs for this locus. The SNP with the highest MAF was selected as a representative  
515 SNP for the hotspot. We defined hotspots as genetic loci with  $\geq 5$  *trans* associations,  
516 yielding a single hotspot for GTEx, 107 for the meQTL and 444 for the eQTLGen data  
517 (Additional File 2, Tables S1 and S2). In [10], the authors provide a total of 114 meQTL  
518 hotspots per our definition. We discarded 7 of the 114 meQTL hotspots (SNPs rs10870226,  
519 rs1570038, rs17420384, rs2295981, rs2685252, rs57743634, rs7924137, as either no *cis* genes  
520 are available or no gene expression data were measured for any of the annotated *cis* genes  
521 (mostly lincRNAs, miRNAs and pseudogenes; Additional File 1, Table S1), which are needed  
522 for locus set definition (see below).

523 **Locus sets.** To mitigate the  $N \ll P$  problem in network inference [4], where the  
524 number of features or parameters far exceeds the number of samples, we run the inference  
525 on a subset of genomic entities (SNPs, genes and CpGs) induced by *trans* hotspots. We  
526 therefore gathered all genes, which could be involved in mediating the observed QTL effects  
527 and thus were considered during the network inference, in the form of *locus sets* for each  
528 hotspot. We bridge the gap between the involved chromosomes by including transcription  
529 factor binding site (TFBS) information collected from *ReMap* [49]<sup>7</sup> and *ENCODE* [50, 51]<sup>8</sup>  
530 as well as human protein-protein interaction (PPI) information available via *theBioGrid* [99]<sup>9</sup>

---

<sup>7</sup>[http://tagc.univ-mrs.fr/remap/download/All/filPeaks\\_public.bed.gz](http://tagc.univ-mrs.fr/remap/download/All/filPeaks_public.bed.gz)

<sup>8</sup><http://hgdownload.cse.ucsc.edu/goldenPath/hg19/encodeDCC/wgEncodeRegTfbsClustered/wgEncodeRegTfbsClusteredWithCellsV3.bed.gz>

<sup>9</sup><https://downloads.thebiogrid.org/Download/BioGRID/Release-Archive/BIOGRID-3.5.166/BIOGRID-ORGANISM-3.5.166.tab2.zip>

531 (version 3.5.166). We filtered *ReMap* and *ENCODE* TFBS for blood related cell types by  
532 selecting all samples which contain at least one of the following terms: "amlpz12\_leukemic",  
533 "amlpz74\_leukemia", "bcell", "bjab", "bl41", "blood", "lcl", "erythroid", "gm", "hbp",  
534 "k562", "kasumi", "lymphoblastoid", "mm1s", "p493", "plasma", "sem", "thp1", "u937".  
535 Genes in the PPI network were filtered for genes expressed in whole blood (GTEx v6p  
536  $RPKM > 0.1$ )<sup>10</sup>. We enumerated all entities to be included in the locus set by performing  
537 the following steps:

- 538 1. Define set  $S_L$  for a locus  $L$  and add the QTL entities (QTL SNP  $\mathcal{S}$  and *trans*-QTL  
539 eGenes/CpGs  $\mathcal{T} = \{T_1, \dots, T_q\}$ , where  $q$  is the number of associated *trans* entities for  
540  $L$ )
- 541 2. Add all genes encoded within 500kb (1Mbp window) of  $\mathcal{S}$  as **SNP-Genes** to  $S_L$  (set  
542  $\mathcal{G}_C$ )
- 543 3. For meQTL hotspots, add genes in the vicinity of each  $T_i \in \mathcal{T}$  (previous, next and  
544 overlapping genes with respect to the location of  $T_i$ ) as **CpG-Genes** to  $S_L$  (set  $\mathcal{G}_T$ )
- 545 4. Add all **TFs** with binding sites within 50bp of each CpG or binding in the promoter  
546 region of each gene over all  $T_i \in \mathcal{T}$  to  $S_L$  (set  $\mathcal{G}_{TF}$ )
- 547 5. Add shortest path genes  $G_{SP}$ , i.e. genes which connect  $\mathcal{G}_C$  (step 2) with  $\mathcal{G}_{TF}$  (step 4)  
548 according to BioGrid PPIs to  $S_L$

549 To define  $G_{SP}$ , we added only genes which reside on the shortest path between the  
550 *trans* entities  $\mathcal{T}$  and the SNP-Genes  $\mathcal{G}_C$  in the induced PPI sub-network, i.e. containing all  
551 genes and their connections which can be linked to either  $\mathcal{G}_C$  or the TFs  $\mathcal{G}_{TF}$ . Specifically,  
552 we added the CpGs to the filtered BioGrid PPI network, connected them to the TFs ( $\mathcal{G}_{TF}$ )

<sup>10</sup>[https://storage.googleapis.com/gtex\\_analysis\\_v6p/rna\\_seq\\_data/GTEX\\_Analysis\\_v6p\\_RNA-seq\\_RNA-SeQCv1.1.8\\_gene\\_rpkms.gct.gz](https://storage.googleapis.com/gtex_analysis_v6p/rna_seq_data/GTEX_Analysis_v6p_RNA-seq_RNA-SeQCv1.1.8_gene_rpkms.gct.gz)

553 which show binding sites in their vicinity and calculated node weights based on network  
554 propagation as described in [10]. We then extracted nodes on paths with maximal total  
555 propagation score based on node-wise propagation scores  $PS$ . For this, we weighted node  
556 scores proportional to  $(-1) \times PS$  and then calculate the minimal node-weight paths between  
557 *trans* entities  $\mathcal{T}$  and SNP-Genes  $\mathcal{G}_C$  using the *sp.between()* method of the *RBGL* R package  
558 (version 1.56.0, R interface to the Boost Graph Library [100]) and extracted all genes on  
559 the resulting shortest paths. All nodes of the generated locus set were subsequently used as  
560 inputs to the network inference.

## 561 **Prior generation**

562 We utilized several data sources to define priors for possible edges between and within dif-  
563 ferent omics levels. Each possible edge between entities in the locus set can only be assigned  
564 a single type of prior. Specifically, the different priors include:

- 565 • **SNP-to-Gene** priors, for edges between the SNP  $\mathcal{S}$  and SNP-Genes  $\mathcal{G}_C$
- 566 • **Gene-to-Gene** priors, for edges between all gene-gene combinations except TFs  $\mathcal{G}_{TF}$   
567 and their eQTL based targets in  $\mathcal{T}$
- 568 • **CpG-to-Gene** priors, for edges between CpGs in  $\mathcal{T}$  and their neighbouring genes  $\mathcal{G}_T$
- 569 • **TF-to-target** priors, for edges between TFs  $\mathcal{G}_{TF}$  and their targets in the *trans* set  $\mathcal{T}$

570

571 **SNP-to-Gene.** To obtain SNP-to-Gene edge priors, we downloaded the full GTEx v6p  
572 whole-blood eQTL table <sup>11</sup>) and calculated, for each SNP-Gene pair, the local false discovery  
573 rate (lFDR, [101]) using the *fdrtool* R package (version 1.2.15). As described in Efron *et al.*

---

<sup>11</sup>file Whole\_Blood\_Analysis.v6p.all\_snpgene\_pairs.txt.gz from <https://www.gtexportal.org/home/datasets>

574 (2008) [101], the lFDR represents the Bayesian posterior probability of having a null case  
575 (i.e. that the null hypothesis is true) given a test statistic. We therefore defined the prior  
576 for a specific SNP  $\mathcal{S}$  and a SNP-Gene  $\mathcal{G}_C$  as  $p_{\mathcal{S}\mathcal{G}_C} = 1 - lFDR_{\mathcal{S}\mathcal{G}_C}$ .

577

578 **Gene-to-Gene.** We formulate *Gene-to-Gene* edge priors by combining public GTEx  
579 gene expression data [38] with PPI information from the BioGrid [99] to retrieve co-expression  
580 p-values and the respective lFDR for pairs of genes connected by a protein - protein interac-  
581 tion. A special case are priors between TFs and their target genes as identified via ChIP-seq  
582 (see above), which are not considered as *Gene-to-Gene* edges but are handled separately as  
583 described under 'TF-to-target priors' below. GTEx v6p RNA-seq gene expression data were  
584 downloaded from the GTEx data portal <sup>12</sup>. Expression data for GTEx were filtered for high  
585 quality samples ( $RIN \geq 6$ ) and log2 transformed, quantile normalized and transferred to  
586 standard normal distribution before removing the first 10 principle components to remove  
587 potential confounding effects [102]. Priors were derived for all Gene-Gene pairs with PPIs in  
588 the BioGRID network, where a gene  $\mathcal{G} \in \mathcal{G}_C \cup \mathcal{G}_{TF}$  (for meQTL) or  $\mathcal{G} \in \mathcal{G}_C \cup \mathcal{G}_{TF} \cup \mathcal{T}$  (for  
589 eQTL). For each pair, we calculated the Pearson correlation p-values in the GTEx expression  
590 data and subsequently determined the lFDR over all p-values. The prior for two genes  $\mathcal{G}_A$   
591 and  $\mathcal{G}_B$  was then set to  $p_{\mathcal{G}_A\mathcal{G}_B} = 1 - lFDR_{\mathcal{G}_A\mathcal{G}_B}$ .

592

593 **CpG-to-Gene.** For the *CpG-to-Gene* priors (meQTL context only), we utilized two  
594 strategies, distinguishing between TF-CpG priors (i.e. priors between CpGs and TFs showing  
595 binding sites near the CpG site, described below under 'TF-to-target priors') and CpG-to-  
596 Gene priors (i.e. where the gene itself is encoded near the CpG). For the *CpG-to-Gene*  
597 priors, we utilized the genome-wide chromHMM [103] states (15 states model) identified in

---

<sup>12</sup><https://www.gtexportal.org/home/datasets>

598 the Roadmap Epigenomics project [40]<sup>13</sup>. These states reflect functional chromatin states in  
 599 200bp windows and were obtained using histone mark combinations as identified via ChIP-  
 600 sequencing. We quantified a CpGs potential to affect a nearby gene,  $p_{T_x}$ , by retrieving the  
 601 proportion of Roadmap cell-lines in which the CpG resides within a transcription start site  
 602 (TSS) related state (see Table 3). We further adjusted the  $p_{T_x}$  by weighting state information  
 603 according to the Houseman blood cell type estimates available from our data. To this end, we  
 604 took the population mean for each of the Houseman cell proportion estimates and multiplied  
 605 them with the chromHMM state proportions. A specific CpG-to-Gene prior for a CpG  $\mathcal{T}_i \in \mathcal{T}$   
 606 and a gene  $\mathcal{G}_{T_i} \in \mathcal{G}_T$  was then set to  $p_{\mathcal{T}_i \mathcal{G}_{T_i}} = p_{T_x}$ , if the genomic distance  $d(\mathcal{T}_i, \mathcal{G}_T) \leq 200bp$ .

STATE NO.	MNEMONIC	DESCRIPTION
<b>1</b>	<b>TssA</b>	<b>Active TSS</b>
<b>2</b>	<b>TssAFlnk</b>	<b>Flanking Active TSS</b>
3	TxFlnk	Transcr. at gene 5' and 3'
4	Tx	Strong transcription
5	TxWk	Weak transcription
6	EnhG	Genic enhancers
7	Enh	Enhancers
8	ZNF/Rpts	ZNF genes & repeats
9	Het	Heterochromatin
<b>10</b>	<b>TssBiv</b>	<b>Bivalent/Poised TSS</b>
<b>11</b>	<b>BivFlnk</b>	<b>Flanking Bivalent TSS/Enh</b>
12	EnhBiv	Bivalent Enhancer
13	ReprPC	Repressed PolyComb
14	ReprPCWk	Weak Repressed PolyComb
15	Quies	Quiescent/Low

Table 3: Description of chromHMM states used in our analyses as given at [https://egg2.wustl.edu/roadmap/web\\_portal/chr\\_state\\_learning.html](https://egg2.wustl.edu/roadmap/web_portal/chr_state_learning.html). Bold faced states were defined as 'active transcription' states and used to set CpG-Gene priors.

607 **TF-to-target priors.** We formulate separate priors for all edges between transcription  
 608 factors  $\mathcal{G}_{TF}$  and *trans* CpGs (meQTL) and *trans* genes (eQTL) in  $\mathcal{T}$ . Priors were only set  
 609 for TF-to-CpG edges where we observe a TF binding site (from ReMap/ENCODE, see above)

<sup>13</sup>obtained from [https://egg2.wustl.edu/roadmap/web\\_portal/chr\\_state\\_learning.html](https://egg2.wustl.edu/roadmap/web_portal/chr_state_learning.html)

610 within 50bp of the CpG. For TF-to-Gene edges, we only considered pairs where the TF has  
611 a binding site 2,000bp upstream and 1,000 downstream of the gene's TSS. In both cases, if  
612 the TFBS criteria are met, we set a fixed large prior of 0.99 for all  $\mathcal{G}_{TF-\mathcal{T}}$  pairs to represent  
613 the strong protein-DNA interaction evidence of ChIP-seq data.

614

615 Finally, the priors for all remaining possible edges which were not set based on one of  
616 the criteria described above, e.g. for SNP-to-Gene edges without eQTL in the GTEx data,  
617 were set to a small pseudo-prior  $p_{pseudo} = 10e^{-7}$ .

## 618 **Ground truth network generation, data simulation and prior ran-** 619 **domization**

We performed a simulation experiment for each of the meQTL hotspots. For each SNP  $\mathcal{S}$  and its corresponding locus set  $\mathcal{S}_L$ , we first collect the corresponding prior matrix  $\mathcal{P}_S$  with priors defined as described above. We generate 10 noisy ( $\mathcal{G}_N$ ) ground truth graphs  $\mathcal{G}_N^{10}, \mathcal{G}_N^{20} \dots \mathcal{G}_N^{100}$  by switching edges in the graph while keeping the degree distribution of a sampled graph  $\mathcal{G}_T$ .  $\mathcal{G}_T$  is generated using all entities of  $\mathcal{S}_L$  by uniformly sampling from  $\mathcal{P}_S$ , i.e.  $\mathcal{G}_T$  contains an edge  $e_{ij}$  for each element  $p_{ij}$  of  $\mathcal{P}_S$ , if  $p_{ij} > p_{pseudo}$  and  $runif(0, 1) \leq p_{ij}$ , where  $runif(0, 1)$  generates uniformly distributed random numbers between [0,1]. This procedure effectively introduces noise in the study. For instance, by switching 10% of the edges from  $\mathcal{G}_T$  to generate  $\mathcal{G}_N^{10}$ , and making sure, that the new edges are not present as priors in  $\mathcal{P}_S$ , we introduce a noise level of 10% when comparing  $\mathcal{P}_S$  to  $\mathcal{G}_N^{10}$ . We simulate data for each  $\mathcal{G}_S \in \{\text{mathpzcG}_T, \mathcal{G}_N^i; i \in \{10, 20, \dots, 100\}\}$  using the *bdgraph.sim()* method of the *BDgraph* package with parameters:  $p=|\mathcal{S}_L|$  (number of nodes),  $\text{graph}=\mathcal{G}_S$ ,  $N=612$  (number of samples in LOLIPOP) and  $\text{mean} = 0$ . This approach generates normally distributed data with a covariance structure as defined by the ground truth graph. We want to assess the impact of

having discrete (genotype) data present for the network inference. To this end, we converted the SNP variable in the simulated data to genotype dosages (0,1,2) reflecting the allele frequencies of the genetic variant used in this simulation run. Specifically, we transformed the Gaussian data obtained from *bdgraph.sim()* to discrete values using the frequencies of the individual dosages for the SNP in the LOLIPOP data as quantile cut points. For each of these simulated data individually, we infer the network models and compare the inferred networks to the respective ground truth graphs  $\mathcal{G}_T, \mathcal{G}_N^{10}, \dots, \mathcal{G}_N^{100}$ . We added one additional comparison, evaluating a prior on the density of the observed graph. For this, we estimated a single prior value reflecting the desired density for all edges based on a binomial model. We use the number of edges  $|E_{\mathcal{G}_T}|$  of all sampled graphs  $\mathcal{G}_T$  for a single run, the total number of possible edges  $|E_T| = (N * (N - 1))/2$ , with  $N$  the total number of available nodes, and set the prior as

$$p_{rbinom} = \max\left(\frac{1}{N_S} * \frac{\sum_{\mathcal{G}_T} |E_{\mathcal{G}_T}|}{|E_T|}, p_{pseudo}\right),$$

620 where  $N_S$  is the number of sampled graphs (i.e. the number of randomizations). For each  
621 hotspot, we repeated the above simulation procedure 100 times to obtain stable results.

## 622 Network inference

623 Based on the data and priors gathered for the individual hotspots, we set out to infer the reg-  
624 ulatory networks which are best supported by these data. We evaluated several state-of-the  
625 art methods with respect to their applicability to this problem, both in a simulation study  
626 (see above) and via replication of inferred networks in real-world data from two large human  
627 population based cohorts. We applied *GeneNet* [45, 104], the graphical lasso [*glasso*, 42],  
628 *BDgraph* [29], *iRafNet* [32] as well as *GENIE3* [46] on the individual data to reconstruct reg-  
629 ulatory networks using the respective *CRAN*<sup>14</sup> and *bioconductor*<sup>15</sup> R packages. An overview

---

<sup>14</sup><https://cran.r-project.org/>

<sup>15</sup><https://www.bioconductor.org/>

630 on the used inference methods and package versions is given in Table 1. Methods were  
631 chosen to reflect a range of different approaches (i.e. shrinkage based partial correlation in  
632 *GeneNet* , Bayesian MCMC sampling in *BDgraph* , lasso in *gLASSO* and tree based in-  
633 ference in *iRafNet* and *GENIE3* ), based on whether or not implementation was readily  
634 available and whether prior knowledge could be incorporated. The well known *GeneNet* and  
635 *GENIE3* methods are not capable of utilizing prior information, but were used as a reference  
636 for comparison to the other methods.

637

638 **GeneNet** For the application of GeneNet we first filtered any CpG probes from the data  
639 containing missing values. We then estimated the regulatory network by calling first the  
640 *ggm.estimate.pcor* followed by the *network.test.edges* and *extract.network* methods, all with  
641 default parameters.

642

643 **GENIE3** To infer networks with GENIE3, we again used the NA filtered data (see above)  
644 with the *GENIE3* method of the package followed by the *getLinkList* method using default  
645 parameters. GENIE3 generates a ranked list of regulatory links which do not relate to any  
646 statistical measure and hence a cutoff for the link weights has to be identified manually<sup>16</sup>.  
647 To define an optimal cutoff, we first divide the list of weights into 200 quantiles (marking  
648 200 distinct cutoffs) if the number of unique link weights exceeded 200. We then extracted  
649 for each cutoff the respective regulatory network and compared it to a scale free topology  
650 analogously to the approach used in [105], generating  $R^2$  values indicating the goodness-of-fit  
651 to the topology. To choose the final network, we followed the approach suggested by Zhang  
652 *et al.* (2005) [105], which suggests to use networks with  $R^2 > 0.8$ . If none of our networks  
653 fit that criteria, we choose the network with the highest  $R^2$ .

654

---

<sup>16</sup>see also <https://bioconductor.org/packages/release/bioc/vignettes/GENIE3/inst/doc/GENIE3.html>



655 **BDgraph** We used BDgraph to infer networks under consideration of prior information  
656 as well as without prior information (*BDgraph* and *BDgraph<sub>P</sub>*) using the *bdgraph* method  
657 of the *BDgraph* CRAN package (version 2.61). The following parameters were set: *method*  
658 = "*gcgm*", *iter* = 10000, *burnin* = 5000. We further set the *g.prior* parameter to the prior  
659 matrix collected for the hotspots and the *g.start* parameter to the incidence matrix obtained  
660 from the prior matrix by setting all entries with prior information  $> 0.5$  to 1 and all others to  
661 0. For comparison with the no prior case, we kept all parameters the same but omitted the  
662 *g.start* and *g.prior* parameters. The graph was then obtained from the fitted model using  
663 the *select* method of the package with parameter *cut* = 0.9, thereby only choosing edges  
664 with a posterior probability of at least 0.9.

665

666 **glasso** Similar to BDgraph, we utilized the graphical lasso both with and without prior  
667 information. To infer the graphical lasso models, we used the *glasso* method available in the  
668 *glasso* CRAN package and set the parameter *penalize.diagonal* = *FALSE*. The *glasso* takes  
669 a regularization parameter  $\lambda$ , which implies either strong penalization of edges (high  $\lambda$ ) or  
670 weak penalization (low  $\lambda$ ) of parameters. This parameter can also be supplied as a matrix  
671  $\Lambda$  of size  $n \times n$  (where  $n$  is the number of nodes/variables) in order to supply individual  
672 parameters for individual edges. We integrated the prior information by first transforming  
673 the prior matrix  $\mathcal{P}$  such that  $\Lambda = 1 - \mathcal{P}$  and then supplying  $\Lambda$  as the regularization  
674 matrix containing values for each possible edge. This approach is similar to what has been  
675 proposed in [30, 31]. In addition, we screened a selection of penalization factors  $\omega$  for both  
676 the prior and the none prior case to construct the optimal graphical lasso network with  
677 respect to the Bayesian Information Criterion (BIC). For the prior case, we included  $\omega$  in  
678 the model by setting  $\Lambda = \Lambda \times \omega$ . For the non-prior case, we set  $\lambda = \omega$ . We performed  
679 5-fold cross validation and inferred the model for all  $\omega \in \{0.01, 0.015, \dots, 1\}$  on the training  
680 set (containing 80% of the data) and then selected the  $\omega$  yielding the minimal mean BIC

681 value on the test data over all folds to generate the final network.

682

683 **iRafNet** We use *iRafNet* to infer networks using prior information (it is not possible to  
684 run it without specifying priors). We called the *iRafNet* method of the package, setting the  
685 parameters  $ntrees = 1000$ ,  $mtry = \text{round}(\text{sqrt}(\text{ncol}(\text{data})-1))$ , and  $npermut = 5$  using the  
686 data filtered for missing values (see above) and then used the *Run\_permutation* method with  
687 the same parameters. The final network was extracted using the *iRafNet\_network* method  
688 by supplying the output of the previous method calls and setting the FDR cutoff parameter  
689  $TH = 0.05$ . We used a custom implementation of *iRafNet* adjusted to make use of multiple  
690 CPUs which we made available at [https://github.com/jhawe/irafnet\\_custom](https://github.com/jhawe/irafnet_custom).

## 691 **Method evaluation via simulation study and cross cohort replication**

692 To identify the inference method best suited for our application, we evaluated all described  
693 network inference methods independently on the simulated data as to 1) their ability to  
694 reconstruct the underlying ground truth network as well as 2) their robustness to noise in  
695 the supplied prior information. We further compared networks inferred independently on the  
696 different cohort data to assess stability of the network inference across different, yet similar,  
697 data. Performance was measured in terms of Matthew's Correlation Coefficient (MCC)  
698 [29, 47, 106] between the inferred networks and the respective ground truth (simulation  
699 study) and the inferred networks on the different cohorts (cross cohort replication). It is  
700 defined as:

$$MCC = \frac{TP \times TN - FP \times FN}{\sqrt{(TP + FP) \times (TP + FN) \times (TN + FP) \times (TN + FN)}} \quad (1)$$

701

702 MCC was calculated using the *compare()* method as implemented in the *BDgraph* package

703 (version 2.61).

## 704 **Transcription factor activities**

705 We calculated transcription factor activities for all TFs extracted from the ReMap/ENCODE  
706 (see above) using the *plsgenomics* R package's *TFA.estimate()* method (version 1.5-2) [107].  
707 As input, we used the full expression matrix from KORA and LOLIPOP individually as well  
708 as the TFBS information encoded as an incidence matrix indicating for each TF its target  
709 genes. Target genes were defined as genes with an TFBS within their promoter region  
710 (2,000bp upstream and 1,000bp downstream of the TSS).

## 711 **Network prioritization and final network creation**

712 Networks were inferred for each of the 107 meQTL and 444 eQTLGen *trans* hotspots with  
713 *gLASSOP* and *BDgraphP*, yielding networks with a median number of 67 and 20 edges  
714 for *gLASSOP* and 72 and 27 for *BDgraphP* over all hotspots, respectively. We filtered and  
715 ranked the networks based on the following criteria.

716 **GWAS filtering.** We filtered genetic loci with hits in genome-wide association studies  
717 (GWAS) using the current version (v1.0.2) of the GWAS catalog [52]. We extracted high  
718 LD (>0.8) SNPs and SNP aliases using the SNiPA tool [53] for each hotspot SNP. If any of  
719 the extracted SNP rsIDs had a match in the GWAS catalog, the hotspot's inferred network  
720 was permitted for downstream analysis.

721 **Network ranking.** We utilized a self devised graph score for prioritizing final models  
722 for further investigation. The graph score reflects desirable biological properties, which can  
723 be assumed for the networks underlying the *trans*-QTL hotspots. The score is formulated  
724 such that 1) the adjacency of SNP-genes and SNPs is rated positively, 2) the presence of  
725 *trans* entities is rated positively if they are not connected directly to the SNP and 3) high

726 graph density is rated negatively (i.e. sparser graphs yield higher scores). Specifically, the  
727 graph score  $S_G$  for an inferred graph  $G$  is defined as:

$$S_G = -\log_{10}(D_G) * \left[ \frac{1}{|\mathcal{G}_C|} \left( \sum_{i=1}^{|G_S|} 1 - \sum_{i=1}^{|\overline{G_S}|} 1 \right) + \frac{1}{|\mathcal{T}|} \left( \sum_{i=1}^{|G_T|} 1 - \sum_{i=1}^{|\overline{G_T}|} 1 \right) \right]$$

728 where:  $D_G$  is the graph density,  $\mathcal{G}_C$  is the set of all SNP-Genes,  $\mathcal{T}$  is the set of all  
729 *trans* entities,  $G_S$  is the set of all SNP-genes adjacent to the SNP in  $G$  or directly connected  
730 to another SNP-Gene,  $\overline{G_S}$  is the set of SNP-Genes in  $G$  but not connected directly to the  
731 SNP or one of the other SNP-Genes,  $G_T$  is the set of *trans* entities in  $G$  which can be  
732 reached from any SNP-Gene without traversing the SNP or another *trans* gene first and  $\overline{G_T}$   
733 is the set of *trans* genes directly connected to the SNP. Only the cluster containing the SNP,  
734 i.e. the SNP itself and any nodes reachable from the SNP via any path in  $G$ , is considered  
735 for calculating  $S_G$ ; if the SNP is not present or no SNP gene has been selected in the final  
736 graph the score is set to 0.

737 In addition to the graph score, we ranked networks according to the total number of  
738 edges and nodes to prioritize smaller networks for detailed analysis.

739 **Graph merging.** Finally, we constructed hotspot networks containing only high con-  
740 fidence edges by merging the individually obtained networks from the two cohorts (KORA  
741 and LOLIPOP) and keeping only edges and nodes present in both networks. Nodes without  
742 any adjacent edges are not included in the final graph.

## 743 Priors for skeletal muscle tissue

744 We downloaded Muscle tissue eQTL generated by Scott *et al.* (2016) [79] from [https://](https://theparkerlab.med.umich.edu/data/papers/doi/10.1038/ncomms11764/)  
745 [theparkerlab.med.umich.edu/data/papers/doi/10.1038/ncomms11764/](https://theparkerlab.med.umich.edu/data/papers/doi/10.1038/ncomms11764/) and used local FDRs  
746 calculated from the provided p-values to define SNP-Gene priors. Gene expression data for  
747 Muscle tissue were obtained from the ARCHS<sup>4</sup> [41] database. We downloaded all relevant

748 Muscle expression data using the keywords "Skeletal\_Muscle" with the ARCHS4 loader<sup>17</sup>  
749 (N=194 samples). Expression data were normalized using the *ComBat* method implemented  
750 in the *sva* R package, providing dataset series ID as batch parameter.

751 *TFBS prediction for muscle tissue.* We used *factorNet* [80] to predict transcription factor  
752 binding sites from DNase-seq chromatin accessibility data obtained from muscle cell lines.  
753 First, we trained a *factorNet* model for all TFs available for the K562 cell-line in ReMap [49].  
754 ReMap ChIP-seq peaks functioned as a ground truth during training, DNase-seq data from  
755 ENCODE<sup>18</sup> [50, 51] and DNA sequence information formed the inputs. We downloaded  
756 DNase-seq data for the LHCN-M2 muscle cell-line from ENCODE in bigWig format for  
757 hg38<sup>19</sup>. *FactorNet* was then run with default parameters, using as input 1) the DNA sequence  
758 and 2) the bigWig DNase track for each of the trained ChIP-seq transcription factors (N=179  
759 TFs from ReMap). High confidence TFBS were extracted by setting a *factorNet* score cutoff  
760 of 0.999, merging overlapping regions and then retaining only regions with a *width* <  $W_{0.95}$ ,  
761 where  $W_{0.95}$  is the 95th percent quantile of the widths of all obtained regions.

## 762 Colocalization analysis

763 GWAS summary statistics for schizophrenia were identified using the GWAS Atlas [108]  
764 <sup>20</sup> and downloaded from [http://walters.psychm.cf.ac.uk/clozuk\\_pgc2.meta.sumstats.txt.gz](http://walters.psychm.cf.ac.uk/clozuk_pgc2.meta.sumstats.txt.gz).  
765 Whole-blood *trans* -eQTL summary statistics for all SNP-Gene pairs from eQTLgen were  
766 downloaded from the eQTLgen website<sup>21</sup>. We used *fastENLOC* [76, 109]<sup>22</sup> to calculate  
767 colocalization probabilities as described in the *fastENLOC* Github README using default  
768 parameters. To generate probabilistic eQTL annotations, we used *DAP-G* [110, 111]<sup>23</sup> and

---

<sup>17</sup>[https://github.com/jhawe/archs4\\_loader](https://github.com/jhawe/archs4_loader)

<sup>18</sup>dataset ENCF971AHO

<sup>19</sup>dataset ENCF639MPM

<sup>20</sup><https://atlas.ctglab.nl/>

<sup>21</sup><https://www.eqtlgen.org/trans-eqtls.html>, file 'Full trans-eQTL summary statistics'

<sup>22</sup><https://github.com/xqwen/fastenloc>

<sup>23</sup><https://github.com/xqwen/dap/>

769 created PIP files as needed using *TORUS* [112]<sup>24</sup>. For LD block definition, we utilized data  
770 available from LDetect [113]<sup>25</sup>.

## 771 **Software environment**

772 In case no other information is given above, all calculations were performed using standard  
773 Unix commands and version 3.5.2 of the R statistical computing language <sup>26</sup> on a Cen-  
774 tos 7 Unix system. The Docker image used in this project is available from dockerhub at  
775 [https://hub.docker.com/repository/docker/jhawe/r3.5.2\\_custom](https://hub.docker.com/repository/docker/jhawe/r3.5.2_custom). The workflows for both  
776 the cohort and the simulation studies were implemented in Snakemake [114] and can be  
777 found on Github at <https://github.com/jhawe/bggm>. All calculations performed to arrive  
778 at the discussed results in this article can be obtained using the code in the pipeline. Data  
779 to run the workflow can be made available upon reasonable request by the authors.

## 780 **Declarations**

### 781 **Availability of data and material**

782 **Data.** All public data information and the respective sources are given in the methods  
783 section, including URLs for downloading the data where possible. The meQTL associations  
784 from Hawe et al. were directly obtained from the supplementary table 3 of the paper [10] and  
785 eQTLGen *trans* -eQTL directly from the eQTLGen browser<sup>27</sup>. The lists of derived hotspots  
786 for both data sets are made available in the supplement of this paper. Cohort data can be  
787 made available upon reasonable request by the authors.

788 **Code.** The complete code used in this project is provided via Github at <https://github.com>.

---

<sup>24</sup><https://github.com/xqwen/torus>

<sup>25</sup><https://bitbucket.org/nygcresearch/ldetect-data/src/master/>

<sup>26</sup><https://www.r-project.org/>

<sup>27</sup><https://eqtlgen.org/trans-eqtls.html>

789 com/jhawe/bggm. The analyses were implemented in the form of a Snakemake pipeline  
790 [114]. The software environment used to calculate the results is available as a Docker im-  
791 age via docker hub at [https://hub.docker.com/repository/docker/jhawe/r3.5.2\\_custom](https://hub.docker.com/repository/docker/jhawe/r3.5.2_custom), the  
792 corresponding dockerfile is available at the project's Github repository.

## 793 **Ethics approval and consent to participate**

794 All KORA participants have given written informed consent and the study was approved  
795 by the Ethics Committee of the Bavarian Medical Association. The LOLIPOP study is  
796 approved by the National Research Ethics Service (07/H0712/150) and all participants gave  
797 written informed consent.

## 798 **Consent for publication**

799 KORA project agreement for this study was granted under K141/15g. The views expressed  
800 are those of the author(s) and not necessarily those of the Imperial College Healthcare NHS  
801 Trust, the NHS, the NIHR or the Department of Health.

## 802 **Competing interests**

803 FJT reports receiving consulting fees from Roche Diagnostics GmbH and Cellarity Inc., and  
804 ownership interest in Cellarity, Inc. and Dermagnostix. The other authors declare that they  
805 have no competing interests.

## 806 **Funding**

807 MH gratefully acknowledges funding by the Federal Ministry of Education and Research  
808 (BMBF, Germany) in the project eMed:confirm (01ZX1708G). JC is supported by the Sin-  
809 gapore Ministry of Health's National Medical Research Council under its Singapore Transla-

810 tional Research Investigator (STaR) Award (NMRC/STaR/0028/2017). AB is supported by  
811 the NIH grant 1R01MH109905. The LOLIPOP study is supported by the National Institute  
812 for Health Research (NIHR) Comprehensive Biomedical Research Centre Imperial College  
813 Healthcare NHS Trust, the NIHR Official Development Assistance (ODA, award 16/136/68),  
814 the European Union FP7 (EpiMigrant, 279143) and H2020 programs (iHealth-T2D, 643774).  
815 The KORA study was initiated and financed by the Helmholtz Zentrum München—German  
816 Research Center for Environmental Health, which is funded by the German Federal Min-  
817 istry of Education and Research (BMBF) and by the State of Bavaria. Furthermore, KORA  
818 research was supported within the Munich Center of Health Sciences (MC-Health), Ludwig-  
819 Maximilians-Universität, as part of LMUinnovativ. The German Diabetes Center is funded  
820 by the German Federal Ministry of Health (Berlin, Germany), the Ministry of Culture and  
821 Science of the state North Rhine-Westphalia (Düsseldorf, Germany), and grants from the  
822 German Federal Ministry of Education and Research (Berlin, Germany) to the German  
823 Center for Diabetes Research e.V. (DZD).

## 824 **Authors' contributions**

825 MH conceived the study, JH performed the analyses. AB and AS assisted with use of GTEx  
826 v8 data. AB and FT contributed to the design of the data analysis strategy. CG, MW, KS,  
827 CH, SK, SW, HP, HG, AP, and MM provided KORA cohort data and JC the LOLIPOP  
828 data. JH and MH wrote the manuscript with input from all authors. All authors read and  
829 approved the final version of the manuscript.

## 830 **Acknowledgements**

831 We thank the participants and research staff of LOLIPOP who made the study possible.  
832 The KORA-Study Group consists of A. Peters (speaker), J. Heinrich, R. Holle, R. Leidl, C.



833 Meisinger, K. Strauch and their co-workers, who are responsible for the design and conduct  
834 of the KORA studies. We gratefully acknowledge the contribution of all members of field  
835 staff conducting the KORA study. Finally, we are grateful to all study participants of KORA  
836 for their invaluable contributions to this study.

## 837 References

- 838 [1] Hasin, Y., Seldin, M., Lusis, A.: Multi-omics approaches to disease. *Genome biology*  
839 **18**(1), 83 (2017). doi:10.1186/s13059-017-1215-1
- 840 [2] Visscher, P.M., Wray, N.R., Zhang, Q., Sklar, P., McCarthy, M.I., Brown, M.A., Yang,  
841 J.: 10 Years of GWAS Discovery: Biology, Function, and Translation. *American Jour-*  
842 *nal of Human Genetics* **101**(1), 5–22 (2017). doi:10.1016/j.ajhg.2017.06.005
- 843 [3] Civelek, M., Lusis, A.J.: Systems genetics approaches to understand complex traits.  
844 *Nature reviews. Genetics* **15**(1), 34–48 (2014). doi:10.1038/nrg3575. NIHMS150003
- 845 [4] Hawe, J.S., Theis, F.J., Heinig, M.: Inferring Interaction Networks From Multi-Omics  
846 Data. *Frontiers in Genetics* **10**, 535 (2019). doi:10.3389/fgene.2019.00535
- 847 [5] Gilad, Y., Rifkin, S.A., Pritchard, J.K.: Revealing the architecture of gene reg-  
848 ulation: the promise of eQTL studies. *Trends in Genetics* **24**(8), 408–415 (2008).  
849 doi:10.1016/J.TIG.2008.06.001
- 850 [6] Joehanes, R., Zhang, X., Huan, T., Yao, C., Ying, S.-x., Nguyen, Q.T., Demirkale,  
851 C.Y., Feolo, M.L., Sharopova, N.R., Sturcke, A., Schäffer, A.A., Heard-Costa, N.,  
852 Chen, H., Liu, P.-c., Wang, R., Woodhouse, K.A., Tanriverdi, K., Freedman, J.E.,  
853 Raghavachari, N., Dupuis, J., Johnson, A.D., O'Donnell, C.J., Levy, D., Munson, P.J.:  
854 Integrated genome-wide analysis of expression quantitative trait loci aids interpretation

855 of genomic association studies. *Genome Biology* **18**(1), 16 (2017). doi:10.1186/s13059-  
856 016-1142-6

857 [7] Vösa, U., Claringbould, A., Westra, H.-j., Bonder, M.J., Zeng, B., Kirsten, H., Saha,  
858 A., Kreuzhuber, R., Kasela, S., Alvaes, I., Fave, M.-j., Agbessi, M., Christiansen, M.,  
859 Verlouw, J., Yaghootkar, H., Sönmez, R., Brown, A., Kukushkina, V., Kalnapenkis,  
860 A., Rüeger, S., Porcu, E., Kronberg-, J., Kettunen, J., Powell, J., Lee, B., Zhang, F.,  
861 Beutner, F., Consortium, B., Brugge, H., Kähönen, M., Kim, Y., Knight, J.C., Kovacs,  
862 P., Krohn, K., Stegle, O., Battle, A., Yang, J., Visscher, P.M., Scholz, M.: Unraveling  
863 the polygenic architecture of complex traits using blood eQTL meta- analysis. *bioRxiv*,  
864 1–57 (2018). doi:10.1101/447367

865 [8] Bonder, M.J., Luijk, R., Zhernakova, D.V., Moed, M., Deelen, P., Vermaat, M., van  
866 Itersson, M., van Dijk, F., van Galen, M., Bot, J., Sliker, R.C., Jhamai, P.M., Verbiest,  
867 M., Suchiman, H.E.D., Verkerk, M., van der Breggen, R., van Rooij, J., Lakenberg, N.,  
868 Arindrarto, W., Kielbasa, S.M., Jonkers, I., van 't Hof, P., Nooren, I., Beekman, M.,  
869 Deelen, J., van Heemst, D., Zhernakova, A., Tigchelaar, E.F., Swertz, M.A., Hofman,  
870 A., Uitterlinden, A.G., Pool, R., van Dongen, J., Hottenga, J.J., Stehouwer, C.D.A.,  
871 van der Kallen, C.J.H., Schalkwijk, C.G., van den Berg, L.H., van Zwet, E.W., Mei,  
872 H., Li, Y., Lemire, M., Hudson, T.J., Slagboom, P.E., Wijmenga, C., Veldink, J.H.,  
873 van Greevenbroek, M.M.J., van Duijn, C.M., Boomsma, D.I., Isaacs, A., Jansen, R.,  
874 van Meurs, J.B.J., 't Hoen, P.A.C., Franke, L., Heijmans, B.T.: Disease variants  
875 alter transcription factor levels and methylation of their binding sites. *Nature Genetics*  
876 **49**(1), 131–138 (2016). doi:10.1038/ng.3721

877 [9] Husquin, L.T., Rotival, M., Fagny, M., Quach, H., Zidane, N., McEwen, L.M.,  
878 MacIsaac, J.L., Kober, M.S., Aschard, H., Patin, E., Quintana-Murci, L.: Ex-  
879 ploring the genetic basis of human population differences in DNA methylation and

- 880 their causal impact on immune gene regulation. *Genome Biology* **19**(1), 222 (2018).  
881 doi:10.1186/s13059-018-1601-3
- 882 [10] Hawe, J.S., Lehne, B.C., Wilson, R., Loh, M., Heinig, M., Gieger, C., Waldenberger,  
883 M., Chambers, J.C.: Genetic variation influencing DNA methylation provides new in-  
884 sights into the molecular pathways regulating genomic function. Manuscript in prepa-  
885 ration (2020)
- 886 [11] West, M.A.L., Kim, K., Kliebenstein, D.J., van Leeuwen, H., Michelmore, R.W., Do-  
887 erge, R.W., Clair, D.A.S.: Global eQTL Mapping Reveals the Complex Genetic Ar-  
888 chitecture of Transcript-Level Variation in Arabidopsis. *Genetics* **175**(3), 1441–1450  
889 (2007). doi:10.1534/GENETICS.106.064972
- 890 [12] Albert, F.W., Bloom, J.S., Siegel, J., Day, L., Kruglyak, L.: Genetics of trans-  
891 regulatory variation in gene expression. *eLife* **7** (2018). doi:10.7554/ELIFE.35471
- 892 [13] Westra, H.-J., Peters, M.J., Esko, T., Yaghootkar, H., Schurmann, C., Kettunen, J.,  
893 Christiansen, M.W., Fairfax, B.P., Schramm, K., Powell, J.E., Zhernakova, A., Zh-  
894 ernakova, D.V., Veldink, J.H., Van den Berg, L.H., Karjalainen, J., Withoff, S., Uit-  
895 terlinden, A.G., Hofman, A., Rivadeneira, F., 't Hoen, P.A.C., Reinmaa, E., Fischer,  
896 K., Nelis, M., Milani, L., Melzer, D., Ferrucci, L., Singleton, A.B., Hernandez, D.G.,  
897 Nalls, M.A., Homuth, G., Nauck, M., Radke, D., Völker, U., Perola, M., Salomaa, V.,  
898 Brody, J., Suchy-Dicey, A., Gharib, S.A., Enquobahrie, D.A., Lumley, T., Montgomery,  
899 G.W., Makino, S., Prokisch, H., Herder, C., Roden, M., Grallert, H., Meitinger, T.,  
900 Strauch, K., Li, Y., Jansen, R.C., Visscher, P.M., Knight, J.C., Psaty, B.M., Ripatti,  
901 S., Teumer, A., Frayling, T.M., Metspalu, A., van Meurs, J.B.J., Franke, L.: System-  
902 atic identification of trans eQTLs as putative drivers of known disease associations.  
903 *Nature Genetics* **45**(10), 1238–1243 (2013). doi:10.1038/ng.2756

- 904 [14] Breitling, R., Li, Y., Tesson, B.M., Fu, J., Wu, C., Wiltshire, T., Gerrits, A., Bystriykh,  
905 L.V., de Haan, G., Su, A.I., Jansen, R.C.: Genetical genomics: spotlight on QTL  
906 hotspots. *PLoS genetics* **4**(10), 1000232 (2008). doi:10.1371/journal.pgen.1000232
- 907 [15] Zhu, J., Zhang, B., Smith, E.N., Drees, B., Brem, R.B., Kruglyak, L., Bumgar-  
908 ner, R.E., Schadt, E.E.: Integrating large-scale functional genomic data to dissect  
909 the complexity of yeast regulatory networks. *Nature Genetics* **40**(7), 854–861 (2008).  
910 doi:10.1038/ng.167
- 911 [16] Ritchie, M.D., Holzinger, E.R., Li, R., Pendergrass, S.A., Kim, D.: Methods of in-  
912 tegrating data to uncover genotype-phenotype interactions. *Nature Reviews Genetics*  
913 **16**(2), 85–97 (2015). doi:10.1038/nrg3868
- 914 [17] Schadt, E.E., Lamb, J., Yang, X., Zhu, J., Edwards, S., Guhathakurta, D., Sieberts,  
915 S.K., Monks, S., Reitman, M., Zhang, C., Lum, P.Y., Leonardson, A., Thieringer,  
916 R., Metzger, J.M., Yang, L., Castle, J., Zhu, H., Kash, S.F., Drake, T.A., Sachs, A.,  
917 Luskis, A.J.: An integrative genomics approach to infer causal associations between  
918 gene expression and disease. *Nature genetics* **37**(7), 710–7 (2005). doi:10.1038/ng1589
- 919 [18] Keurentjes, J.J.B., Fu, J., Terpstra, I.R., Garcia, J.M., Van Den Ackerveken, G., Snoek,  
920 L.B., Peeters, A.J.M., Vreugdenhil, D., Koornneef, M., Jansen, R.C.: Regulatory net-  
921 work construction in *Arabidopsis* by using genome-wide gene expression quantitative  
922 trait loci. *Proceedings of the National Academy of Sciences of the United States of*  
923 *America* **104**(5), 1708–1713 (2007). doi:10.1073/pnas.0610429104
- 924 [19] Luijk, R., Dekkers, K.F., van Iterson, M., Arindrarto, W., Claringbould, A., Hop, P.,  
925 Boomsma, D.I., van Duijn, C.M., van Greevenbroek, M.M.J., Veldink, J.H., Wijmenga,  
926 C., Franke, L., 't Hoen, P.A.C., Jansen, R., van Meurs, J., Mei, H., Slagboom, P.E.,  
927 Heijmans, B.T., van Zwet, E.W.: Genome-wide identification of directed gene networks

- 928 using large-scale population genomics data. *Nature Communications* **9**(1), 3097 (2018).  
929 doi:10.1038/s41467-018-05452-6
- 930 [20] Mine, K.L., Shulzhenko, N., Yambartsev, A., Rochman, M., Sanson, G.F.O., Lando,  
931 M., Varma, S., Skinner, J., Volfovsky, N., Deng, T., Brenna, S.M.F., Carvalho,  
932 C.R.N., Ribalta, J.C.L., Bustin, M., Matzinger, P., Silva, I.D.C.G., Lyng, H., Gerbase-  
933 DeLima, M., Morgun, A.: Gene network reconstruction reveals cell cycle and antiviral  
934 genes as major drivers of cervical cancer. *Nature communications* **4**, 1806 (2013).  
935 doi:10.1038/NCOMMS2693
- 936 [21] Bonneau, R., Reiss, D.J., Shannon, P., Facciotti, M., Hood, L., Baliga, N.S., Thorsson,  
937 V.: The inferelator: An algorithm for learning parsimonious regulatory networks from  
938 systems-biology data sets de novo. *Genome Biology* **7**(5) (2006). doi:10.1186/gb-2006-  
939 7-5-r36
- 940 [22] Lam, K.Y., Westrick, Z.M., Müller, C.L., Christiaen, L., Bonneau, R.: Fused Re-  
941 gression for Multi-source Gene Regulatory Network Inference. *PLoS Computational*  
942 *Biology* **12**(12), 1–23 (2016). doi:10.1371/journal.pcbi.1005157
- 943 [23] Suhre, K., Arnold, M., Bhagwat, A.M., Cotton, R.J., Engelke, R., Raffler, J., Sarwath,  
944 H., Thareja, G., Wahl, A., DeLisle, R.K., Gold, L., Pezer, M., Lauc, G., El-Din Selim,  
945 M.A., Mook-Kanamori, D.O., Al-Dous, E.K., Mohamoud, Y.A., Malek, J., Strauch,  
946 K., Grallert, H., Peters, A., Kastenmüller, G., Gieger, C., Graumann, J.: Connecting  
947 genetic risk to disease end points through the human blood plasma proteome. *Nature*  
948 *Communications* **8**, 14357 (2017). doi:10.1038/ncomms14357
- 949 [24] Castro, J.C., Valdés, I., Gonzalez-García, L.N., Danies, G., Cañas, S., Winck, F.V.,  
950 Núñez, C.E., Restrepo, S., Riaño-Pachón, D.M.: Gene regulatory networks on trans-  
951 fer entropy (GRNTE): A novel approach to reconstruct gene regulatory interactions

952 applied to a case study for the plant pathogen *Phytophthora infestans*. Theoretical  
953 Biology and Medical Modelling **16**(1), 1–15 (2019). doi:10.1186/s12976-019-0103-7

954 [25] Kamoun, A., Idbaih, A., Dehais, C., Elarouci, N., Carpentier, C., Letouzé, E., Colin,  
955 C., Mokhtari, K., Jouvét, A., Uro-Coste, E., Martin-Duverneuil, N., Sanson, M., Delat-  
956 tre, J.-Y., Figarella-Branger, D., de Reyniès, A., Ducray, F., Adam, C., Andraud, M.,  
957 Aubriot-Lorton, M.-H., Bauchet, L., Beauchesne, P., Bielle, F., Blechet, C., Campone,  
958 M., Carpentier, A.F., Carpiuc, I., Cazals-Hatem, D., Chenard, M.-P., Chiforeanu, D.,  
959 Chinot, O., Cohen-Moyal, E., Colin, P., Dam-Hieu, P., Desenclos, C., Desse, N., Dher-  
960 main, F., Diebold, M.-D., Eimer, S., Faillot, T., Fesneau, M., Fontaine, D., Gaillard,  
961 S., Gauchotte, G., Gaultier, C., Ghiringhelli, F., Godard, J., Gueye, E.M., Guillamo,  
962 J.S., Hamdi-Elouadhani, S., Honnorat, J., Kemeny, J.L., Khallil, T., Labrousse, F.,  
963 Langlois, O., Laquerriere, A., Larrieu-Ciron, D., Lechapt-Zalcman, E., Guérinel, C.L.,  
964 Levillain, P.-M., Loiseau, H., Loussouarn, D., Maurage, C.-A., Menei, P., Motsuo  
965 Fotso, M.J., Noel, G., Parker, F., Peoc'h, M., Polivka, M., Quintin-Roué, I., Ramirez,  
966 C., Ricard, D., Richard, P., Rigau, V., Rousseau, A., Runavot, G., Sevestre, H., Tortel,  
967 M.C., Vandenbos, F., Vauleon, E., Viennet, G., Villa, C., Villa, C.: Integrated multi-  
968 omics analysis of oligodendroglial tumours identifies three subgroups of 1p/19q co-  
969 deleted gliomas. Nature Communications **7**, 11263 (2016). doi:10.1038/ncomms11263

970 [26] Huang, S., Chaudhary, K., Garmire, L.X.: More Is Better: Recent Progress  
971 in Multi-Omics Data Integration Methods. Frontiers in genetics **8**, 84 (2017).  
972 doi:10.3389/fgene.2017.00084

973 [27] Greenfield, A., Hafemeister, C., Bonneau, R.: Robust data-driven incorporation of  
974 prior knowledge into the inference of dynamic regulatory networks. Bioinformatics  
975 **29**(8), 1060–1067 (2013). doi:10.1093/bioinformatics/btt099

- 976 [28] Christley, S., Nie, Q., Xie, X.: Incorporating Existing Network Information into Gene  
977 Network Inference. *PLoS ONE* **4**(8), 6799 (2009). doi:10.1371/journal.pone.0006799
- 978 [29] Mohammadi, A., Wit, E.C.: Bayesian Structure Learning in Sparse Gaussian Graphi-  
979 cal Models. *Bayesian Analysis* **10**(1), 109–138 (2015). doi:10.1214/14-BA889
- 980 [30] Wang, Z., Xu, W., Lucas, F.A.S., Liu, Y.: Incorporating prior knowl-  
981 edge into Gene Network Study. *Bioinformatics* **29**(20), 2633–2640 (2013).  
982 doi:10.1093/bioinformatics/btt443
- 983 [31] Li, Y., Jackson, S.A.: Gene Network Reconstruction by Integration of Prior Biological  
984 Knowledge. *G3 (Bethesda, Md.)* **5**(6), 1075–9 (2015). doi:10.1534/g3.115.018127
- 985 [32] Petralia, F., Wang, P., Yang, J., Tu, Z.: Integrative random forest  
986 for gene regulatory network inference. *Bioinformatics* **31**(12), 197–205 (2015).  
987 doi:10.1093/bioinformatics/btv268
- 988 [33] Zuo, Y., Cui, Y., Yu, G., Li, R., Resson, H.W.: Incorporating prior biological  
989 knowledge for network-based differential gene expression analysis using differentially  
990 weighted graphical LASSO. *BMC Bioinformatics* **18**(1), 99 (2017). doi:10.1186/s12859-  
991 017-1515-1
- 992 [34] Studham, M.E., Tjärnberg, A., Nordling, T.E.M., Nelander, S., Sonnhammer, E.L.L.:  
993 Functional association networks as priors for gene regulatory network inference. *Bioin-  
994 formatics* **30**(12), 130–138 (2014). doi:10.1093/bioinformatics/btu285
- 995 [35] Gustafsson, M., Hörnquist, M.: Gene expression prediction by soft integration and the  
996 elastic net - Best performance of the DREAM3 gene expression challenge. *PLoS ONE*  
997 **5**(2) (2010). doi:10.1371/journal.pone.0009134

- 998 [36] Siahpirani, A.F., Roy, S.: A prior-based integrative framework for functional tran-  
999 scriptional regulatory network inference. *Nucleic Acids Research* **45**(4), 1–22 (2017).  
1000 doi:10.1093/nar/gkw963
- 1001 [37] Pei, B., Shin, D.G.: Reconstruction of biological networks by incorporating prior  
1002 knowledge into bayesian network models. *Journal of Computational Biology* **19**(12),  
1003 1324–1334 (2012). doi:10.1089/cmb.2011.0194
- 1004 [38] The GTEx Consortium: The Genotype-Tissue Expression (GTEx) pilot anal-  
1005 ysis: Multitissue gene regulation in humans. *Science* **348**, 648–660 (2015).  
1006 doi:10.1126/science.1262110
- 1007 [39] Aguet, F., Brown, A.A., Castel, S.E., Davis, J.R., He, Y., Jo, B., Mohammadi, P.,  
1008 Park, Y.S., Parsana, P., Segrè, A.V., Strober, B.J., Zappala, Z., Cummings, B.B.,  
1009 Gelfand, E.T., Hadley, K., Huang, K.H., Lek, M., Li, X., Nedzel, J.L., Nguyen, D.Y.,  
1010 Noble, M.S., Sullivan, T.J., Tukiainen, T., MacArthur, D.G., Getz, G., Addington, A.,  
1011 Guan, P., Koester, S., Little, A.R., Lockhart, N.C., Moore, H.M., Rao, A., Struewing,  
1012 J.P., Volpi, S., Brigham, L.E., Hasz, R., Hunter, M., Johns, C., Johnson, M., Kopen,  
1013 G., Leinweber, W.F., Lonsdale, J.T., McDonald, A., Mestichelli, B., Myer, K., Roe,  
1014 B., Salvatore, M., Shad, S., Thomas, J.A., Walters, G., Washington, M., Wheeler, J.,  
1015 Bridge, J., Foster, B.A., Gillard, B.M., Karasik, E., Kumar, R., Miklos, M., Moser,  
1016 M.T., Jewell, S.D., Montroy, R.G., Rohrer, D.C., Valley, D., Mash, D.C., Davis, D.A.,  
1017 Sobin, L., Barcus, M.E., Branton, P.A., Abell, N.S., Balliu, B., Delaneau, O., Frésard,  
1018 L., Gamazon, E.R., Garrido-Martín, D., Gewirtz, A.D.H., Gliner, G., Gloudemans,  
1019 M.J., Han, B., He, A.Z., Hormozdiari, F., Li, X., Liu, B., Kang, E.Y., McDowell, I.C.,  
1020 Ongen, H., Palowitch, J.J., Peterson, C.B., Quon, G., Ripke, S., Saha, A., Shabalin,  
1021 A.A., Shimko, T.C., Sul, J.H., Teran, N.A., Tsang, E.K., Zhang, H., Zhou, Y.H.,  
1022 Bustamante, C.D., Cox, N.J., Guigó, R., Kellis, M., McCarthy, M.I., Conrad, D.F.,



- 1023 Eskin, E., Li, G., Nobel, A.B., Sabatti, C., Stranger, B.E., Wen, X., Wright, F.A.,  
1024 Ardlie, K.G., Dermitzakis, E.T., Lappalainen, T., Battle, A., Brown, C.D., Engelhardt,  
1025 B.E., Montgomery, S.B., Handsaker, R.E., Kashin, S., Karczewski, K.J., Nguyen, D.T.,  
1026 Trowbridge, C.A., Barshir, R., Basha, O., Bogu, G.K., Chen, L.S., Chiang, C., Damani,  
1027 F.N., Ferreira, P.G., Hall, I.M., Howald, C., Im, H.K., Kim, Y., Kim-Hellmuth, S.,  
1028 Mangul, S., Monlong, J., Muñoz-Aguirre, M., Ndungu, A.W., Nicolae, D.L., Oliva,  
1029 M., Panousis, N., Papasaikas, P., Payne, A.J., Quan, J., Reverter, F., Sammeth, M.,  
1030 Scott, A.J., Sodaiei, R., Stephens, M., Urbut, S., Van De Bunt, M., Wang, G., Xi,  
1031 H.S., Yeger-Lotem, E., Zaugg, J.B., Akey, J.M., Bates, D., Chan, J., Claussnitzer,  
1032 M., Demanelis, K., Diegel, M., Doherty, J.A., Feinberg, A.P., Fernando, M.S., Halow,  
1033 J., Hansen, K.D., Haugen, E., Hickey, P.F., Hou, L., Jasmine, F., Jian, R., Jiang,  
1034 L., Johnson, A., Kaul, R., Kibriya, M.G., Lee, K., Li, J.B., Li, Q., Lin, J., Lin, S.,  
1035 Linder, S., Linke, C., Liu, Y., Maurano, M.T., Molinie, B., Nelson, J., Neri, F.J.,  
1036 Park, Y., Pierce, B.L., Rinaldi, N.J., Rizzardi, L.F., Sandstrom, R., Skol, A., Smith,  
1037 K.S., Snyder, M.P., Stamatoyannopoulos, J., Tang, H., Wang, L., Wang, M., Van  
1038 Wittenberghe, N., Wu, F., Zhang, R., Nierras, C.R., Carithers, L.J., Vaught, J.B.,  
1039 Gould, S.E., Lockart, N.C., Martin, C., Addington, A.M., Koester, S.E., Undale, A.H.,  
1040 Smith, A.M., Tabor, D.E., Roche, N.V., McLean, J.A., Vatanian, N., Robinson, K.L.,  
1041 Valentino, K.M., Qi, L., Hunter, S., Hariharan, P., Singh, S., Um, K.S., Matose,  
1042 T., Tomaszewski, M.M., Barker, L.K., Mosavel, M., Siminoff, L.A., Traino, H.M.,  
1043 Flicek, P., Juettemann, T., Ruffier, M., Sheppard, D., Taylor, K., Trevanion, S.J.,  
1044 Zerbino, D.R., Craft, B., Goldman, M., Haeussler, M., Kent, W.J., Lee, C.M., Paten,  
1045 B., Rosenbloom, K.R., Vivian, J., Zhu, J.: Genetic effects on gene expression across  
1046 human tissues. *Nature* **550**(7675), 204–213 (2017). doi:10.1038/nature24277
- 1047 [40] The Roadmap Epigenomics Consortium: Integrative analysis of 111 reference human  
1048 epigenomes. *Nature* **518**(7539), 317–330 (2015). doi:10.1038/nature14248

- 1049 [41] Lachmann, A., Torre, D., Keenan, A.B., Jagodnik, K.M., Lee, H.J., Wang, L., Silver-  
1050 stein, M.C., Ma'ayan, A.: Massive mining of publicly available RNA-seq data from  
1051 human and mouse. *Nature Communications* **9**(1), 1366 (2018). doi:10.1038/s41467-  
1052 018-03751-6
- 1053 [42] Friedman, J., Hastie, T., Tibshirani, R.: Sparse inverse covariance estimation with the  
1054 graphical lasso. *Biostatistics* **9**(3), 432–441 (2008). doi:10.1093/biostatistics/kxm045
- 1055 [43] Pfeiffer, L., Wahl, S., Pilling, L.C., Reischl, E., Sandling, J.K., Kunze, S., Holdt, L.M.,  
1056 Kretschmer, A., Schramm, K., Adamski, J., Klopp, N., Illig, T., Hedman, Å.K., Roden,  
1057 M., Hernandez, D.G., Singleton, A.B., Thasler, W.E., Grallert, H., Gieger, C., Herder,  
1058 C., Teupser, D., Meisinger, C., Spector, T.D., Kronenberg, F., Prokisch, H., Melzer,  
1059 D., Peters, A., Deloukas, P., Ferrucci, L., Waldenberger, M.: DNA methylation of  
1060 lipid-related genes affects blood lipid levels. *Circulation. Cardiovascular genetics* **8**(2),  
1061 334–42 (2015). doi:10.1161/CIRCGENETICS.114.000804
- 1062 [44] Chambers, J.C., Loh, M., Lehne, B., Drong, A., Kriebel, J., Motta, V., Wahl, S.,  
1063 Elliott, H.R., Rota, F., Scott, W.R., Zhang, W., Tan, S.T., Campanella, G., Chadeau-  
1064 Hyam, M., Yengo, L., Richmond, R.C., Adamowicz-Brice, M., Afzal, U., Bozaoglu,  
1065 K., Mok, Z.Y., Ng, H.K., Pattou, F., Prokisch, H., Rozario, M.A., Tarantini, L.,  
1066 Abbott, J., Ala-Korpela, M., Albetti, B., Ammerpohl, O., Bertazzi, P.A., Blancher,  
1067 C., Caiazzo, R., Danesh, J., Gaunt, T.R., de Lusignan, S., Gieger, C., Illig, T., Jha,  
1068 S., Jones, S., Jowett, J., Kangas, A.J., Kasturiratne, A., Kato, N., Kotea, N., Kow-  
1069 lessur, S., Pitkäniemi, J., Punjabi, P., Saleheen, D., Schafmayer, C., Soininen, P.,  
1070 Tai, E.S., Thorand, B., Tuomilehto, J., Wickremasinghe, A.R., Kyrtopoulos, S.A.,  
1071 Aitman, T.J., Herder, C., Hampe, J., Cauchi, S., Relton, C.L., Froguel, P., Soong,  
1072 R., Vineis, P., Jarvelin, M.R., Scott, J., Grallert, H., Bollati, V., Elliott, P., Mc-  
1073 Carthy, M.I., Kooner, J.S.: Epigenome-wide association of DNA methylation markers

- 1074 in peripheral blood from Indian Asians and Europeans with incident type 2 diabetes:  
1075 A nested case-control study. *The Lancet Diabetes and Endocrinology* **3**(7), 526–534  
1076 (2015). doi:10.1016/S2213-8587(15)00127-8
- 1077 [45] Opgen-Rhein, R., Strimmer, K.: From correlation to causation networks: A simple  
1078 approximate learning algorithm and its application to high-dimensional plant gene  
1079 expression data. *BMC Systems Biology* **1**(1), 37 (2007). doi:10.1186/1752-0509-1-37
- 1080 [46] Huynh-Thu, V.A., Irrthum, A., Wehenkel, L., Geurts, P.: Inferring Regulatory Net-  
1081 works from Expression Data Using Tree-Based Methods. *PLoS ONE* **5**(9), 12776  
1082 (2010). doi:10.1371/journal.pone.0012776
- 1083 [47] Matthews, B.W.: Comparison of the predicted and observed secondary structure of T4  
1084 phage lysozyme. *BBA - Protein Structure* (1975). doi:10.1016/0005-2795(75)90109-9
- 1085 [48] Arrieta-Ortiz, M.L., Hafemeister, C., Bate, A.R., Chu, T., Greenfield, A., Shuster, B.,  
1086 Barry, S.N., Gallitto, M., Liu, B., Kacmarczyk, T., Santoriello, F., Chen, J., Rodrigues,  
1087 C.D.A., Sato, T., Rudner, D.Z., Driks, A., Bonneau, R., Eichenberger, P.: An exper-  
1088 imentally supported model of the *Bacillus subtilis* global transcriptional regulatory  
1089 network. *Molecular systems biology* **11**(11), 839 (2015). doi:10.15252/msb.20156236
- 1090 [49] Chèneby, J., Gheorghe, M., Artufel, M., Mathelier, A., Ballester, B.: ReMap  
1091 2018: An updated atlas of regulatory regions from an integrative analysis of DNA-  
1092 binding ChIP-seq experiments. *Nucleic Acids Research* **46**(D1), 267–275 (2018).  
1093 doi:10.1093/nar/gkx1092
- 1094 [50] ENCODE Project Consortium: An integrated encyclopedia of DNA elements in the  
1095 human genome. *Nature* **489**(7414), 57–74 (2012). doi:10.1038/nature11247
- 1096 [51] Davis, C.A., Hitz, B.C., Sloan, C.A., Chan, E.T., Davidson, J.M., Gabdank, I.,  
1097 Hilton, J.A., Jain, K., Baymuradov, U.K., Narayanan, A.K., Onate, K.C., Graham,

- 1098 K., Miyasato, S.R., Dreszer, T.R., Strattan, J.S., Jolanki, O., Tanaka, F.Y., Cherry,  
1099 J.M.: The Encyclopedia of DNA elements (ENCODE): data portal update. *Nucleic  
1100 acids research* **46**(D1), 794–801 (2018). doi:10.1093/nar/gkx1081
- 1101 [52] Buniello, A., MacArthur, J.A., Cerezo, M., Harris, L.W., Hayhurst, J., Malangone,  
1102 C., McMahon, A., Morales, J., Mountjoy, E., Sollis, E., Suveges, D., Vrousitou, O.,  
1103 Whetzel, P.L., Amode, R., Guillen, J.A., Riat, H.S., Trevanion, S.J., Hall, P., Junk-  
1104 ins, H., Flicek, P., Burdett, T., Hindorff, L.A., Cunningham, F., Parkinson, H.: The  
1105 NHGRI-EBI GWAS Catalog of published genome-wide association studies, targeted  
1106 arrays and summary statistics 2019. *Nucleic Acids Research* **47**(D1), 1005–1012 (2019).  
1107 doi:10.1093/nar/gky1120
- 1108 [53] Arnold, M., Raffler, J., Pfeufer, A., Suhre, K., Kastenmüller, G.: SNiPA: An inter-  
1109 active, genetic variant-centered annotation browser. *Bioinformatics* **31**(8), 1334–1336  
1110 (2015). doi:10.1093/bioinformatics/btu779
- 1111 [54] Goes, F.S., McGrath, J., Avramopoulos, D., Wolyniec, P., Pirooznia, M., Ruczinski,  
1112 I., Nestadt, G., Kenny, E.E., Vacic, V., Peters, I., Lencz, T., Darvasi, A., Mulle,  
1113 J.G., Warren, S.T., Pulver, A.E.: Genome-wide association study of schizophrenia  
1114 in Ashkenazi Jews. *American Journal of Medical Genetics Part B: Neuropsychiatric  
1115 Genetics* **168**(8), 649–659 (2015). doi:10.1002/ajmg.b.32349
- 1116 [55] de Jong, S., van Eijk, K.R., Zeegers, D.W.L.H., Strengman, E., Janson, E.,  
1117 Veldink, J.H., van den Berg, L.H., Cahn, W., Kahn, R.S., Boks, M.P.M., Ophoff,  
1118 R.A., PGC Schizophrenia (GWAS) Consortium, T.P.S.G.: Expression QTL analy-  
1119 sis of top loci from GWAS meta-analysis highlights additional schizophrenia can-  
1120 didate genes. *European journal of human genetics : EJHG* **20**(9), 1004–8 (2012).  
1121 doi:10.1038/ejhg.2012.38

- 1122 [56] Kanazawa, T., Bousman, C.A., Liu, C., Everall, I.P.: Schizophrenia genetics in the  
1123 genome-wide era: A review of Japanese studies. *npj Schizophrenia* **3**(1), 2–7 (2017).  
1124 doi:10.1038/s41537-017-0028-2
- 1125 [57] Saito, T., Ikeda, M., Mushiroda, T., Ozeki, T., Kondo, K., Shimasaki, A., Kawase,  
1126 K., Hashimoto, S., Yamamori, H., Yasuda, Y., Fujimoto, M., Ohi, K., Takeda, M.,  
1127 Kamatani, Y., Numata, S., Ohmori, T., ichi Ueno, S., Makinodan, M., Nishihata,  
1128 Y., Kubota, M., Kimura, T., Kanahara, N., Hashimoto, N., Fujita, K., Nemoto, K.,  
1129 Fukao, T., Suwa, T., Noda, T., Yada, Y., Takaki, M., Kida, N., Otsuru, T., Murakami,  
1130 M., Takahashi, A., Kubo, M., Hashimoto, R., Iwata, N.: Pharmacogenomic Study of  
1131 Clozapine-Induced Agranulocytosis/Granulocytopenia in a Japanese Population. *Bio-*  
1132 *logical Psychiatry* **80**(8), 636–642 (2016). doi:10.1016/j.biopsych.2015.12.006
- 1133 [58] Rustenhoven, J., Smith, A.M., Smyth, L.C., Jansson, D., Scotter, E.L., Swanson,  
1134 M.E.V., Aalderink, M., Coppieters, N., Narayan, P., Handley, R., Overall, C., Park,  
1135 T.I.H., Schweder, P., Heppner, P., Curtis, M.A., Faull, R.L.M., Dragunow, M.: PU.1  
1136 regulates Alzheimer’s disease-associated genes in primary human microglia. *Molecular*  
1137 *neurodegeneration* **13**(1), 44 (2018). doi:10.1186/s13024-018-0277-1
- 1138 [59] Hu, Z., Gu, X., Baraoidan, K., Ibanez, V., Sharma, A., Kadkol, S., Munker, R., Acker-  
1139 man, S., Nucifora, G., Sauntharajah, Y.: RUNX1 regulates corepressor interactions  
1140 of PU.1. *Blood* **117**(24), 6498–508 (2011). doi:10.1182/blood-2010-10-312512
- 1141 [60] Watanabe, Y., Nunokawa, A., Kaneko, N., Muratake, T., Arinami, T., Ujike, H.,  
1142 Inada, T., Iwata, N., Kunugi, H., Itokawa, M., Otowa, T., Ozaki, N., Someya, T.:  
1143 Two-stage case–control association study of polymorphisms in rheumatoid arthritis sus-  
1144 ceptibility genes with schizophrenia. *Journal of Human Genetics* **54**(1), 62–65 (2009).  
1145 doi:10.1038/jhg.2008.4

- 1146 [61] Schizophrenia Psychiatric Genome-Wide Association Study (GWAS) Consortium,  
1147 T.S.P.G.-W.A.S.G.: Genome-wide association study identifies five new schizophrenia  
1148 loci. *Nature genetics* **43**(10), 969–76 (2011). doi:10.1038/ng.940
- 1149 [62] Shi, J., Levinson, D.F., Duan, J., Sanders, A.R., Zheng, Y., Pe'er, I., Dudbridge, F.,  
1150 Holmans, P.A., Whittemore, A.S., Mowry, B.J., Olincy, A., Amin, F., Cloninger, C.R.,  
1151 Silverman, J.M., Buccola, N.G., Byerley, W.F., Black, D.W., Crowe, R.R., Oksenberg,  
1152 J.R., Mirel, D.B., Kendler, K.S., Freedman, R., Gejman, P.V.: Common variants  
1153 on chromosome 6p22.1 are associated with schizophrenia. *Nature* **460**(7256), 753–7  
1154 (2009). doi:10.1038/nature08192
- 1155 [63] International Schizophrenia Consortium, I.S., Purcell, S.M., Wray, N.R., Stone, J.L.,  
1156 Visscher, P.M., O'Donovan, M.C., Sullivan, P.F., Sklar, P.: Common polygenic vari-  
1157 ation contributes to risk of schizophrenia and bipolar disorder. *Nature* **460**(7256),  
1158 748–52 (2009). doi:10.1038/nature08185
- 1159 [64] Stefansson, H., Ophoff, R.A., Steinberg, S., Andreassen, O.A., Cichon, S., Rujescu, D.,  
1160 Werge, T., Pietiläinen, O.P.H., Mors, O., Mortensen, P.B., Sigurdsson, E., Gustafsson,  
1161 O., Nyegaard, M., Tuulio-Henriksson, A., Ingason, A., Hansen, T., Suvisaari, J.,  
1162 Lonnqvist, J., Paunio, T., Børglum, A.D., Hartmann, A., Fink-Jensen, A., Nordentoft,  
1163 M., Hougaard, D., Norgaard-Pedersen, B., Böttcher, Y., Olesen, J., Breuer, R., Möller,  
1164 H.-J., Giegling, I., Rasmussen, H.B., Timm, S., Mattheisen, M., Bitter, I., Réthelyi,  
1165 J.M., Magnusdottir, B.B., Sigmundsson, T., Olason, P., Masson, G., Gulcher, J.R.,  
1166 Haraldsson, M., Fossdal, R., Thorgeirsson, T.E., Thorsteinsdottir, U., Ruggeri, M.,  
1167 Tosato, S., Franke, B., Strengman, E., Kiemeneý, L.A., Genetic Risk and Outcome in  
1168 Psychosis (GROUP), Melle, I., Djurovic, S., Abramova, L., Kaleda, V., Sanjuan, J.,  
1169 de Frutos, R., Bramon, E., Vassos, E., Fraser, G., Ettinger, U., Picchioni, M., Walker,  
1170 N., Touloupoulou, T., Need, A.C., Ge, D., Yoon, J.L., Shianna, K.V., Freimer, N.B.,

- 1171 Cantor, R.M., Murray, R., Kong, A., Golimbet, V., Carracedo, A., Arango, C., Costas,  
1172 J., Jönsson, E.G., Terenius, L., Agartz, I., Petursson, H., Nöthen, M.M., Rietschel, M.,  
1173 Matthews, P.M., Muglia, P., Peltonen, L., St Clair, D., Goldstein, D.B., Stefansson, K.,  
1174 Collier, D.A.: Common variants conferring risk of schizophrenia. *Nature* **460**(7256),  
1175 744–7 (2009). doi:10.1038/nature08186
- 1176 [65] Quednow, B.B., Brinkmeyer, J., Mobascher, A., Nothnagel, M., Musso, F., Grün-  
1177 der, G., Savary, N., Petrovsky, N., Frommann, I., Lennertz, L., Spreckelmeyer, K.N.,  
1178 Wienker, T.F., Dahmen, N., Thuerauf, N., Clepce, M., Kiefer, F., Majic, T., Möss-  
1179 ner, R., Maier, W., Gallinat, J., Diaz-Lacava, A., Toliat, M.R., Thiele, H., Nürnberg,  
1180 P., Wagner, M., Winterer, G.: Schizophrenia risk polymorphisms in the TCF4 gene  
1181 interact with smoking in the modulation of auditory sensory gating. *Proceedings of*  
1182 *the National Academy of Sciences of the United States of America* **109**(16), 6271–6  
1183 (2012). doi:10.1073/pnas.1118051109
- 1184 [66] Zweier, C., Peippo, M.M., Hoyer, J., Sousa, S., Bottani, A., Clayton-Smith, J., Rear-  
1185 don, W., Saraiva, J., Cabral, A., Göhring, I., Devriendt, K., de Ravel, T., Bijlsma,  
1186 E.K., Hennekam, R.C.M., Orrico, A., Cohen, M., Dreweke, A., Reis, A., Nürnberg,  
1187 P., Rauch, A.: Haploinsufficiency of TCF4 Causes Syndromal Mental Retardation  
1188 with Intermittent Hyperventilation (Pitt-Hopkins Syndrome). *The American Journal*  
1189 *of Human Genetics* **80**(5), 994–1001 (2007). doi:10.1086/515583
- 1190 [67] Jung, M., Häberle, B.M., Tschakowsky, T., Wittmann, M.-T., Balta, E.-A., Stadler,  
1191 V.-C., Zweier, C., Dörfler, A., Gloeckner, C.J., Lie, D.C.: Analysis of the expression  
1192 pattern of the schizophrenia-risk and intellectual disability gene TCF4 in the devel-  
1193 oping and adult brain suggests a role in development and plasticity of cortical and  
1194 hippocampal neurons. *Molecular autism* **9**, 20 (2018). doi:10.1186/s13229-018-0200-1

- 1195 [68] Huo, Y., Li, S., Liu, J., Li, X., Luo, X.-J.: Functional genomics reveal gene regulatory  
1196 mechanisms underlying schizophrenia risk. *Nature Communications* **10**(1), 670 (2019).  
1197 doi:10.1038/s41467-019-08666-4
- 1198 [69] Roussos, P., Katsel, P., Davis, K.L., Giakoumaki, S.G., Lencz, T., Malhotra, A.K.,  
1199 Siever, L.J., Bitsios, P., Haroutunian, V.: Convergent findings for abnormalities of  
1200 the NF- $\kappa$ B signaling pathway in schizophrenia. *Neuropsychopharmacology : official*  
1201 *publication of the American College of Neuropsychopharmacology* **38**(3), 533–9 (2013).  
1202 doi:10.1038/npp.2012.215
- 1203 [70] Saia-Cereda, V.M., Cassoli, J.S., Schmitt, A., Falkai, P., Nascimento, J.M., Martins-de-  
1204 Souza, D.: Proteomics of the corpus callosum unravel pivotal players in the dysfunction  
1205 of cell signaling, structure, and myelination in schizophrenia brains. *European Archives*  
1206 *of Psychiatry and Clinical Neuroscience* **265**(7), 601–612 (2015). doi:10.1007/s00406-  
1207 015-0621-1
- 1208 [71] Bagyinszky, E., Youn, Y.C., An, S.S.A., Kim, S.: The genetics of Alzheimer’s disease.  
1209 *Clinical interventions in aging* **9**, 535–51 (2014). doi:10.2147/CIA.S51571
- 1210 [72] Dowdle, W.E., Robinson, J.F., Kneist, A., Sierrol-Piquer, M.S., Frints, S.G.M., Corbit,  
1211 K.C., Zaghoul, N.A., van Lijnschoten, G., Mulders, L., Verver, D.E., Zerres, K., Reed,  
1212 R.R., Attié-Bitach, T., Johnson, C.A., García-Verdugo, J.M., Katsanis, N., Bergmann,  
1213 C., Reiter, J.F., Reiter, J.F.: Disruption of a Ciliary B9 Protein Complex Causes  
1214 Meckel Syndrome. *The American Journal of Human Genetics* **89**(1), 94–110 (2011).  
1215 doi:10.1016/j.ajhg.2011.06.003
- 1216 [73] Stuart, M.J., Singhal, G., Baune, B.T.: Systematic review of the neurobiological  
1217 relevance of chemokines to psychiatric disorders. *Frontiers in Cellular Neuroscience*  
1218 **9**(September), 1–15 (2015). doi:10.3389/fncel.2015.00357



- 1219 [74] Sanchez, E., Darvish, H., Mesias, R., Taghavi, S., Firouzabadi, S.G., Walker, R.H.,  
1220 Tafakhori, A., Paisán-Ruiz, C.: Identification of a Large DNAJB2 Deletion in a Family  
1221 with Spinal Muscular Atrophy and Parkinsonism. *Human mutation* **37**(11), 1180–1189  
1222 (2016). doi:10.1002/humu.23055
- 1223 [75] Rodriguez, M.S., Egaña, I., Lopitz-Otsoa, F., Aillet, F., Lopez-Mato, M.P., Dor-  
1224 ronroso, A., Lobato-Gil, S., Sutherland, J.D., Barrio, R., Trigueros, C., Lang, V.:  
1225 The RING ubiquitin E3 RNF114 interacts with A20 and modulates NF- $\kappa$ B activity  
1226 and T-cell activation. *Cell Death and Disease* **5**(8) (2014). doi:10.1038/cddis.2014.366
- 1227 [76] Wen, X., Pique-Regi, R., Luca, F.: Integrating molecular QTL data into genome-wide  
1228 genetic association analysis: Probabilistic assessment of enrichment and colocalization.  
1229 *PLOS Genetics* **13**(3), 1006646 (2017). doi:10.1371/journal.pgen.1006646
- 1230 [77] Pardiñas, A.F., Holmans, P., Pocklington, A.J., Escott-Price, V., Ripke, S., Carrera,  
1231 N., Legge, S.E., Bishop, S., Cameron, D., Hamshere, M.L., Han, J., Hubbard, L.,  
1232 Lynham, A., Mantripragada, K., Rees, E., MacCabe, J.H., McCarroll, S.A., Baune,  
1233 B.T., Breen, G., Byrne, E.M., Dannlowski, U., Eley, T.C., Hayward, C., Martin, N.G.,  
1234 McIntosh, A.M., Plomin, R., Porteous, D.J., Wray, N.R., Caballero, A., Geschwind,  
1235 D.H., Huckins, L.M., Ruderfer, D.M., Santiago, E., Sklar, P., Stahl, E.A., Won, H.,  
1236 Agerbo, E., Als, T.D., Andreassen, O.A., Bækvad-Hansen, M., Mortensen, P.B., Peder-  
1237 sen, C.B., Børghlum, A.D., Bybjerg-Grauholm, J., Djurovic, S., Durmishi, N., Pedersen,  
1238 M.G., Golimbet, V., Grove, J., Hougaard, D.M., Mattheisen, M., Molden, E., Mors, O.,  
1239 Nordentoft, M., Pejovic-Milovancevic, M., Sigurdsson, E., Silagadze, T., Hansen, C.S.,  
1240 Stefansson, K., Stefansson, H., Steinberg, S., Tosato, S., Werge, T., Harold, D., Sims,  
1241 R., Gerrish, A., Chapman, J., Abraham, R., Hollingworth, P., Pahwa, J., Denning, N.,  
1242 Thomas, C., Taylor, S., Powell, J., Proitsi, P., Lupton, M., Lovestone, S., Passmore,  
1243 P., Craig, D., McGuinness, B., Johnston, J., Todd, S., Maier, W., Jessen, F., Heun, R.,

- 1244 Schurmann, B., Ramirez, A., Becker, T., Herold, C., Lacour, A., Drichel, D., Nothen,  
1245 M., Goate, A., Cruchaga, C., Nowotny, P., Morris, J.C., Mayo, K., O'Donovan, M.,  
1246 Owen, M., Williams, J., Achilla, E., Barr, C.L., Böttger, T.W., Cohen, D., Curran,  
1247 S., Dempster, E., Dima, D., Sabes-Figuera, R., Flanagan, R.J., Frangou, S., Frank,  
1248 J., Gasse, C., Gaughran, F., Giegling, I., Hannon, E., Hartmann, A.M., Heißenker, B.,  
1249 Helthuis, M., Horsdal, H.T., Ingimarsson, O., Jollie, K., Kennedy, J.L., Köhler, O.,  
1250 Konte, B., Lang, M., Lewis, C., MacCaba, J., Malhotra, A.K., McCrone, P., Meier,  
1251 S.M., Mill, J., Nöthen, M.M., Pedersen, C.B., Rietschel, M., Rujescu, D., Schwalber,  
1252 A., Sørensen, H.J., Spencer, B., Støvring, H., Strohmaier, J., Sullivan, P., Vassos,  
1253 E., Verbelen, M., Collier, D.A., Kirov, G., Owen, M.J., O'Donovan, M.C., Walters,  
1254 J.T.R.: Common schizophrenia alleles are enriched in mutation-intolerant genes and  
1255 in regions under strong background selection. *Nature Genetics* **50**(3), 381–389 (2018).  
1256 doi:10.1038/s41588-018-0059-2
- 1257 [78] The Genotype Tissue Expression Consortium: The GTEx Consortium atlas of genetic  
1258 regulatory effects across human tissues The Genotype Tissue Expression Consortium.  
1259 bioRxiv (2019). doi:10.1101/787903
- 1260 [79] Scott, L.J., Erdos, M.R., Huyghe, J.R., Welch, R.P., Beck, A.T., Wolford, B.N.,  
1261 Chines, P.S., Didion, J.P., Narisu, N., Stringham, H.M., Taylor, D.L., Jackson,  
1262 A.U., Vadlamudi, S., Bonnycastle, L.L., Kinnunen, L., Saramies, J., Sundvall, J.,  
1263 Albanus, R.D., Kiseleva, A., Hensley, J., Crawford, G.E., Jiang, H., Wen, X., Watanabe,  
1264 R.M., Lakka, T.A., Mohlke, K.L., Laakso, M., Tuomilehto, J., Koistinen, H.A.,  
1265 Boehnke, M., Collins, F.S., Parker, S.C.J.: The genetic regulatory signature of type  
1266 2 diabetes in human skeletal muscle. *Nature Communications* **7**(1), 11764 (2016).  
1267 doi:10.1038/ncomms11764
- 1268 [80] Quang, D., Xie, X.: FactorNet: A deep learning framework for predicting cell type spe-

- 1269 cific transcription factor binding from nucleotide-resolution sequential data. *Methods*  
1270 (November 2018), 1–8 (2019). doi:10.1016/j.ymeth.2019.03.020
- 1271 [81] Singh, A.N., Gasman, B.: Disentangling the genetics of sarcopenia: prioritization of  
1272 NUDT3 and KLF5 as genes for lean mass & HLA-DQB1-AS1 for hand grip strength  
1273 with the associated enhancing SNPs & a scoring system. *BMC Medical Genetics* **21**(1),  
1274 40 (2020). doi:10.1186/s12881-020-0977-6
- 1275 [82] Oishi, Y., Manabe, I., Tobe, K., Ohsugi, M., Kubota, T., Fujiu, K., Maemura, K.,  
1276 Kubota, N., Kadowaki, T., Nagai, R.: SUMOylation of Krüppel-like transcription  
1277 factor 5 acts as a molecular switch in transcriptional programs of lipid metabolism  
1278 involving PPAR- $\delta$ . *Nature Medicine* **14**(6), 656–666 (2008). doi:10.1038/nm1756
- 1279 [83] Moresi, V., Carrer, M., Grueter, C.E., Rifki, O.F., Shelton, J.M., Richardson, J.A.,  
1280 Bassel-Duby, R., Olson, E.N.: Histone deacetylases 1 and 2 regulate autophagy flux and  
1281 skeletal muscle homeostasis in mice. *Proceedings of the National Academy of Sciences*  
1282 of the United States of America **109**(5), 1649–54 (2012). doi:10.1073/pnas.1121159109
- 1283 [84] Silverstein, R.A., Ekwall, K.: Sin3: a flexible regulator of global gene expression and  
1284 genome stability. *Current Genetics* **47**(1), 1–17 (2005). doi:10.1007/s00294-004-0541-5
- 1285 [85] Lee, T.I., Young, R.A.: Transcription of Eukaryotic Protein-Coding Genes. *Annual*  
1286 *Review of Genetics* **34**(1), 77–137 (2000). doi:10.1146/annurev.genet.34.1.77
- 1287 [86] Zhang, J., Bang, M.-L., Gokhin, D.S., Lu, Y., Cui, L., Li, X., Gu, Y., Dalton, N.D.,  
1288 Scimia, M.C., Peterson, K.L., Lieber, R.L., Chen, J.: Syncoilin is required for gener-  
1289 ating maximum isometric stress in skeletal muscle but dispensable for muscle cytoar-  
1290 chitecture. *American journal of physiology. Cell physiology* **294**(5), 1175–82 (2008).  
1291 doi:10.1152/ajpcell.00049.2008

- 1292 [87] Brown, S.C., Torelli, S., Ugo, I., De Biasia, F., Howman, E.V., Poon, E., Britton, J.,  
1293 Davies, K.E., Muntoni, F.: Syncoilin upregulation in muscle of patients with neuro-  
1294 muscular disease. *Muscle & Nerve* **32**(6), 715–725 (2005). doi:10.1002/mus.20431
- 1295 [88] Seim, I., Jeffery, P.L., Chopin, L.K.: Gene expression profiling of The Cancer Genome  
1296 Atlas supports an inverse association between body mass index (BMI) and major  
1297 oesophageal tumour subtypes. *bioRxiv*, 378778 (2018). doi:10.1101/378778
- 1298 [89] Oldknow, K., Morton, N.M., Yadav, M., Rajoanah, S., Huesa, C., Bungler, L., Fer-  
1299 ron, M., Karsenty, G., MacRae, V., Milan, J.L., Farquharson, C.: An emerging  
1300 role of phospho1 in the regulation of energy metabolism. *Bone Abstracts* (2013).  
1301 doi:10.1530/boneabs.01.OC6.6
- 1302 [90] Mittelstraß, K., Waldenberger, M.: DNA methylation in human lipid metabolism  
1303 and related diseases. *Current Opinion in Lipidology* **29**(2), 116–124 (2018).  
1304 doi:10.1097/MOL.0000000000000491
- 1305 [91] Wahl, S., Drong, A., Lehne, B., Loh, M., Scott, W.R., Kunze, S., Tsai, P.-C., Ried,  
1306 J.S., Zhang, W., Yang, Y., Tan, S., Fiorito, G., Franke, L., Guarrera, S., Kasela, S.,  
1307 Kriebel, J., Richmond, R.C., Adamo, M., Afzal, U., Ala-Korpela, M., Albetti, B.,  
1308 Ammerpohl, O., Apperley, J.F., Beekman, M., Bertazzi, P.A., Black, S.L., Blancher,  
1309 C., Bonder, M.-J., Brosch, M., Carstensen-Kirberg, M., de Craen, A.J.M., de Lusignan,  
1310 S., Dehghan, A., Elkalaawy, M., Fischer, K., Franco, O.H., Gaunt, T.R., Hampe, J.,  
1311 Hashemi, M., Isaacs, A., Jenkinson, A., Jha, S., Kato, N., Krogh, V., Laffan, M.,  
1312 Meisinger, C., Meitinger, T., Mok, Z.Y., Motta, V., Ng, H.K., Nikolakopoulou, Z.,  
1313 Nteliopoulos, G., Panico, S., Pervjakova, N., Prokisch, H., Rathmann, W., Roden,  
1314 M., Rota, F., Rozario, M.A., Sandling, J.K., Schafmayer, C., Schramm, K., Siebert,  
1315 R., Slagboom, P.E., Soininen, P., Stolk, L., Strauch, K., Tai, E.-S., Tarantini, L.,

- 1316 Thorand, B., Tigchelaar, E.F., Tumino, R., Uitterlinden, A.G., van Duijn, C., van  
1317 Meurs, J.B.J., Vineis, P., Wickremasinghe, A.R., Wijmenga, C., Yang, T.-P., Yuan,  
1318 W., Zhernakova, A., Batterham, R.L., Smith, G.D., Deloukas, P., Heijmans, B.T.,  
1319 Herder, C., Hofman, A., Lindgren, C.M., Milani, L., van der Harst, P., Peters, A.,  
1320 Illig, T., Relton, C.L., Waldenberger, M., Jarvelin, M.-R., Bollati, V., Soong, R.,  
1321 Spector, T.D., Scott, J., McCarthy, M.I., Elliott, P., Bell, J.T., Matullo, G., Gieger,  
1322 C., Kooner, J.S., Grallert, H., Chambers, J.C.: Epigenome-wide association study of  
1323 body mass index , and the adverse outcomes of adiposity. *Nature* **541**(7635), 81–86  
1324 (2017). doi:10.1038/nature20784.Epigenome-wide
- 1325 [92] Pietrobelli, A., Lee, R.C., Capristo, E., Deckelbaum, R.J., Heymsfield, S.B.: An inde-  
1326 pendent, inverse association of high-density-lipoprotein-cholesterol concentration with  
1327 nonadipose body mass. *The American Journal of Clinical Nutrition* **69**(4), 614–620  
1328 (1999). doi:10.1093/ajcn/69.4.614
- 1329 [93] Dayeh, T., Tuomi, T., Almgren, P., Perflyev, A., Jansson, P.-A., de Mello,  
1330 V.D., Pihlajamäki, J., Vaag, A., Groop, L., Nilsson, E., Ling, C.: DNA methy-  
1331 lation of loci within *ABCG1* and *PHOSPHO1* in blood DNA  
1332 is associated with future type 2 diabetes risk. *Epigenetics* **11**(7), 482–488 (2016).  
1333 doi:10.1080/15592294.2016.1178418
- 1334 [94] Wang, G., Padmanabhan, S., Miyamoto-Mikami, E., Fuku, N., Tanaka, M., Miyachi,  
1335 M., Murakami, H., Cheng, Y.-C., Mitchell, B.D., Austin, K.G., Pitsiladis, Y.P.: Gwas  
1336 of elite jamaican, african american and japanese sprint athletes: 2254 may 30, 945 am  
1337 - 1000 am. *Medicine & Science in Sports & Exercise* **46**(5S) (2014)
- 1338 [95] Weber, L.M., Saelens, W., Cannoodt, R., Soneson, C., Hapfelmeier, A., Gardner, P.P.,  
1339 Boulesteix, A.-L., Saeys, Y., Robinson, M.D.: Essential guidelines for computational

- 1340 method benchmarking. *Genome Biology* **20**(1), 125 (2019). doi:10.1186/s13059-019-  
1341 1738-8
- 1342 [96] Schramm, K., Marzi, C., Schurmann, C., Carstensen, M., Reinmaa, E., Biffar, R.,  
1343 Eckstein, G., Gieger, C., Grabe, H.-J., Homuth, G., Kastenmüller, G., Mägi, R.,  
1344 Metspalu, A., Mihailov, E., Peters, A., Petersmann, A., Roden, M., Strauch, K.,  
1345 Suhre, K., Teumer, A., Völker, U., Völzke, H., Wang-Sattler, R., Waldenberger, M.,  
1346 Meitinger, T., Illig, T., Herder, C., Grallert, H., Prokisch, H.: Mapping the ge-  
1347 netic architecture of gene regulation in whole blood. *PloS one* **9**(4), 93844 (2014).  
1348 doi:10.1371/journal.pone.0093844
- 1349 [97] Holle, R., Happich, M., Löwel, H., Wichmann, H.E.: KORA - A research plat-  
1350 form for population based health research. *Gesundheitswesen* **67**(SUPPL. 1) (2005).  
1351 doi:10.1055/s-2005-858235
- 1352 [98] Lehne, B., Drong, A.W., Loh, M., Zhang, W., Scott, W.R., Tan, S.-T., Afzal, U.,  
1353 Scott, J., Jarvelin, M.-R., Elliott, P., McCarthy, M.I., Kooner, J.S., Chambers, J.C.:  
1354 A coherent approach for analysis of the Illumina HumanMethylation450 BeadChip  
1355 improves data quality and performance in epigenome-wide association studies. *Genome*  
1356 *Biology* **16**(1), 37 (2015). doi:10.1186/s13059-015-0600-x
- 1357 [99] Oughtred, R., Stark, C., Breitkreutz, B.-J., Rust, J., Boucher, L., Chang, C., Ko-  
1358 las, N., O'Donnell, L., Leung, G., McAdam, R., Zhang, F., Dolma, S., Willems, A.,  
1359 Coulombe-Huntington, J., Chatr-Aryamontri, A., Dolinski, K., Tyers, M.: The Bi-  
1360 oGRID interaction database: 2019 update. *Nucleic acids research* **47**(D1), 529–541  
1361 (2019). doi:10.1093/nar/gky1079
- 1362 [100] Siek, J., Lee, L.-Q., Lumsdaine, A.: *The Boost Graph Library - User Guide and*  
1363 *Reference Manual*. Addison-Wesley, Amsterdam (2002)

- 1364 [101] Efron, B., *et al.*: Microarrays, empirical bayes and the two-groups model. *Statistical*  
1365 *science* **23**(1), 1–22 (2008)
- 1366 [102] Parsana, P., Ruberman, C., Jaffe, A.E., Schatz, M.C., Battle, A., Leek, J.T.: Address-  
1367 ing confounding artifacts in reconstruction of gene co-expression networks. *Genome*  
1368 *Biology* **20**(1), 94 (2019). doi:10.1186/s13059-019-1700-9
- 1369 [103] Ernst, J., Kellis, M.: ChromHMM: automating chromatin-state discovery and charac-  
1370 terization. *Nature Methods* **9**(3), 215–216 (2012). doi:10.1038/nmeth.1906
- 1371 [104] Schäfer, J., Strimmer, K.: An empirical Bayes approach to inferring large-  
1372 scale gene association networks. *Bioinformatics* **21**(6), 754–764 (2004).  
1373 doi:10.1093/bioinformatics/bti062. [https://academic.oup.com/bioinformatics/article-](https://academic.oup.com/bioinformatics/article-pdf/21/6/754/506488/bti062.pdf)  
1374 [pdf/21/6/754/506488/bti062.pdf](https://academic.oup.com/bioinformatics/article-pdf/21/6/754/506488/bti062.pdf)
- 1375 [105] Zhang, B., Horvath, S.: A General Framework for Weighted Gene Co-Expression Net-  
1376 work Analysis. *Statistical Applications in Genetics and Molecular Biology* **4**(1) (2005).  
1377 doi:10.2202/1544-6115.1128. arXiv:1403.6652v2
- 1378 [106] Chicco, D., Jurman, G.: The advantages of the Matthews correlation coefficient (MCC)  
1379 over F1 score and accuracy in binary classification evaluation. *BMC Genomics* **21**(1),  
1380 1–13 (2020). doi:10.1186/s12864-019-6413-7
- 1381 [107] Boulesteix, A.-L., Strimmer, K.: Predicting transcription factor activities from com-  
1382 bined analysis of microarray and ChIP data: a partial least squares approach. *Theo-*  
1383 *retical biology & medical modelling* **2**, 23 (2005). doi:10.1186/1742-4682-2-23
- 1384 [108] Watanabe, K., Stringer, S., Frei, O., Umićević Mirkov, M., de Leeuw, C., Polderman,  
1385 T.J.C., van der Sluis, S., Andreassen, O.A., Neale, B.M., Posthuma, D.: A global  
1386 overview of pleiotropy and genetic architecture in complex traits. *Nature Genetics*  
1387 **51**(9), 1339–1348 (2019). doi:10.1038/s41588-019-0481-0

- 1388 [109] Pividori, M., Rajagopal, P.S., Barbeira, A.N., Liang, Y., Melia, O., Bastarache,  
1389 L., Park, Y., Consortium, T.G., Wen, X., Im, H.K.: PhenomeXcan: Mapping  
1390 the genome to the phenome through the transcriptome. *bioRxiv*, 833210 (2019).  
1391 doi:10.1101/833210
- 1392 [110] Wen, X., Lee, Y., Luca, F., Pique-Regi, R.: Efficient Integrative Multi-SNP Association  
1393 Analysis via Deterministic Approximation of Posteriors. *American Journal of Human  
1394 Genetics* **98**(6), 1114–1129 (2016). doi:10.1016/j.ajhg.2016.03.029
- 1395 [111] Lee, Y., Luca, F., Pique-Regi, R., Wen, X.: Bayesian Multi-SNP Genetic Associa-  
1396 tion Analysis: Control of FDR and Use of Summary Statistics. *bioRxiv*, 1–46 (2018).  
1397 doi:10.1101/316471
- 1398 [112] Wen, X.: Effective QTL Discovery Incorporating Genomic Annotations. *bioRxiv*,  
1399 032003 (2015). doi:10.1101/032003
- 1400 [113] Berisa, T., Pickrell, J.K.: Approximately independent linkage disequilib-  
1401 rium blocks in human populations. *Bioinformatics* **32**(2), 283–285 (2016).  
1402 doi:10.1093/bioinformatics/btv546
- 1403 [114] Köster, J., Rahmann, S.: Snakemake—a scalable bioinformatics workflow engine. *Bioin-  
1404 formatics* **28**(19), 2520–2522 (2012). doi:10.1093/bioinformatics/bts480